Structure-Based Design, Synthesis, and Study of Potent Inhibitors of β-Ketoacyl-acyl Carrier Protein Synthase III as Potential Antimicrobial Agents

Zhe Nie,*,† Carin Perretta,† Jia Lu,‡ Ying Su,§ Stephen Margosiak,‡ Ketan S. Gajiwala,§ Joseph Cortez,‡ Victor Nikulin,† Kraig M. Yager,† Krzysztof Appelt, and Shaosong Chu*,†

Departments of Medicinal Chemistry, Protein Biochemistry and Structural Biology, Quorex Pharmaceuticals, Inc., 1890 Rutherford Road, Suite 200, Carlsbad, California 92008

Received October 26, 2004

Fatty acid biosynthesis is essential for bacterial survival. Components of this biosynthetic pathway have been identified as attractive targets for the development of new antibacterial agents. FabH, β-ketoacyl-ACP synthase III, is a particularly attractive target, since it is central to the initiation of fatty acid biosynthesis and is highly conserved among Gram-positive and -negative bacteria. Small molecules that inhibit FabH enzymatic activity have the potential to be candidates within a novel class of selective, nontoxic, broad-spectrum antibacterials. Using crystallographic structural information on these highly conserved active sites and structure based drug design principles, a benzoylaminobenzoic acid series of compounds was developed as potent inhibitors of FabH. This inhibitor class demonstrates strong antibacterial activity against Gram-positive and selected Gram-negative organisms.

Introduction

Fatty acid biosynthesis (FAB) is an essential metabolic process for prokaryotic organisms and is required for cell viability and growth.[1] Targeting this pathway consequently represents a reasonable approach for developing new antibacterial agents. Since many of today's nosochomial bacterial infections are resistant to several of the available antibiotics, compounds targeting the FAB pathway could fill a serious medical need. Large multifunction proteins termed type I fatty acid synthases catalyze these essential reactions in eukaryotes.[2] In contrast, bacteria use multiple enzymes to accomplish the same goal and are referred to as type II, or dissociated, fatty acid synthases.[3] The bacterial system and proteins bear little homology to the human system and therefore represent a set of attractive target proteins for novel antibacterial development. Indeed, this pathway has been targeted previously by both natural products (e.g., cerulenin and thiolactomycin) and the synthetic derivatives (e.g., triclosan, isoniazid, and the diazoborines) that inhibit the condensation enzymes and the enoyl-ACP reductase activity of the FabI gene product, respectively. Unfortunately, these agents and/or associated targets have various shortcomings and are of limited usefulness in the development of broad-spectrum antimicrobials.[4]

A key enzyme responsible for initiation of bacterial fatty acid biosynthesis has so far escaped serious attention by the drug discovery industry. FabH, a β-keto-acyl-ACP synthase, is the bacterial condensing enzyme in Gram-positive and -negative bacteria that initiates the FAB cycle by catalyzing the first condensation step between acetyl-CoA and malonyl-ACP (Figure 1).[5] The other bacterial condensing enzymes FabB and FabF, functioning later in the cycle, differ significantly from FabH in that they use acyl-ACP rather than acetyl-CoA as the primer for subsequent condensations and are hence nonredundant. As a result, no other known enzyme in the pathway appears to be able to accomplish this essential reaction, and thus, FabH appears to play a key role in the bacterial FAB cycle. FabH proteins from both Gram-positive and -negative bacteria are highly conserved at the sequence and structural level while there are no significantly homologous proteins in humans. Importantly, the residues that comprise the active site are essentially invariant among Gram-positive and -negative organisms. These attributes suggest that small molecule inhibitors of FabH enzymatic activity could be potential development candidates leading to selective, nontoxic, and broad-spectrum antibacterials.

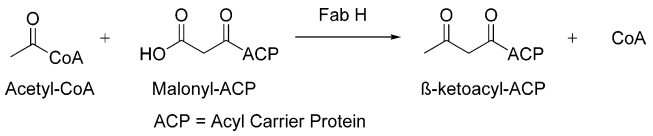

Figure 1. FabH-catalyzed initiation reaction of fatty acid biosynthesis.

Herein we describe the structure-based drug design approach that facilitated generation of potent FabH inhibitors with strong antibacterial activity against Gram-positive and selected Gram-negative organisms. This process was initiated using proprietary computational methods to pare down the more than 3 million commercial chemicals available from reputable commercial sources to generate a FabH-directed compound library. These sets of compounds were screened in enzymatic assays to generate leads that were cocrystallized with various pathogenic FabH proteins and subsequently optimized using structure-guided drug design methods.

* Corresponding author. Current address: Phoenix Pharmacologics, Inc. Phone: 858-452-6688 ext 109. E-mail: zhenie@phoenixpharmaco.com.
† Medicinal Chemistry.
‡ Protein Biochemistry.
§ Structural Biology.

10.1021/jm049141s CCC: $30.25
Published on Web 02/12/2005

Scheme 1[a]

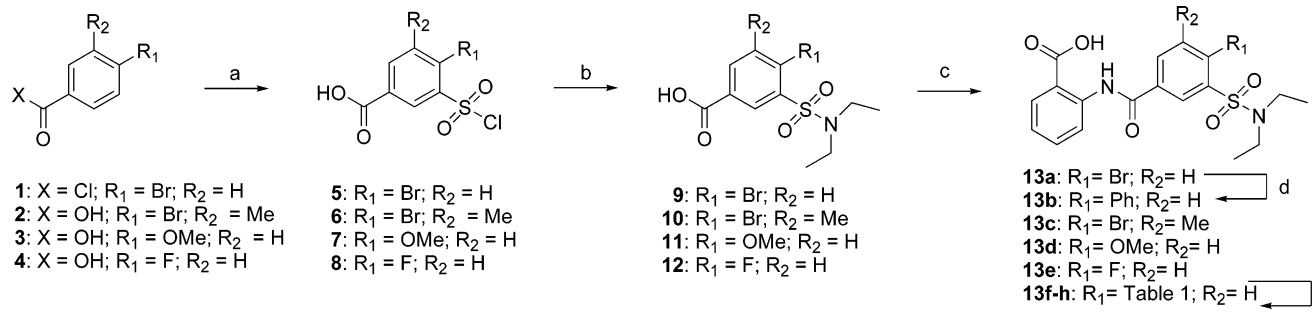

[a] Reagents: (a) $ClSO_3H$, 65−140 °C; (b) $HNEt_2$, EtOAc; (c) (i) $SOCl_2$, DMF (cat.), reflux; (ii) methyl anthranilate, pyr; (iii) NaOH, THF/MeOH; (d) $PhB(OH)_2$, $Pd(PPh_3)_4$, aq Na_2CO_3, DME, reflux; (e) amine or alcohol, K_2CO_3 or NaH, DMF, rt or heat.

In Silico Selection of a FabH-Directed Compound Library

Target-based approaches were used for selecting the initial compound library destined for screening. To apply target-based selection criteria, all available information concerning FabH was collected. This knowledge was then translated into various search queries in order to mine chemical databases for compounds with an increased potential to bind the FabH active site. Specifically, known inhibitors,[6−8] substrates, and the active site topology from available FabH crystal structures[9−12] were used to build FabH-specific queries. Compound selection proceeded via searches of substructure, 2D similarity, phamacophore with size and shape constraints, and docking with FlexX (Tripos, Inc.). The pharmacophore models describe specific areas for desired protein−ligand interactions and limit the molecular volume to be appropriate for the FabH active site. The commercial compound database was prefiltered to remove members that did not satisfy Lipinski's guidelines[13] and that contained undesirable groups that could potentially generate false positives due to reactivity and aggregation.[14,15] After applying these criteria and methods, ~2500 compounds from the prefiltered commercial database were selected for initial FabH inhibition screening.

Biological Methods

The potency of FabH inhibition (IC_{50}) was determined using [^{3}H]- or [^{14}C]-radiolabeled substrates. This was accomplished at fixed concentrations of acetyl-CoA in a coupled FabD/FabH assay system that generates the substrate malonyl-ACP in situ. Subsequently, the FabH acetylation reaction was performed to exclude the possible contribution of undesired FabD inhibitory activity. Compounds with an $IC_{50} < 10$ μM and good aqueous solubility were included in cocrystallization trials with *Entercoccus faecalis* and *Haemophilus influenzae* FabH proteins and the derived protein−inhibitor cocrystal structures were used to further optimize the inhibitors.

Biochemical screening of the 2500 select compound library resulted in 27 hits with $IC_{50} < 10$ μM. Of the four structurally diverse series identified, the benzoylaminobenzoic acid series of compounds was chosen for optimization. The MIC (minimum inhibitory concentration) of sufficiently potent compounds was assessed using both Gram-positive and -negative pathogenic bacteria.

Chemistry

Syntheses of diethylsulfonamide derivatives (**13a**−**h**) began from commercially available substituted benzoic acids or benzoyl chlorides (**1**−**4**) using procedures described in the literature (Scheme 1).[16] As expected, *p*-bromo derivatives (**1** and **2**) and *p*-fluoro derivative **4** required much higher temperatures (140 °C vs 65 °C) to achieve chlorosulfonylation as compared to *p*-methoxy derivative **3**. Subsequent reaction with diethylamine provided diethylsulfonamide derivatives (**9**−**12**). The desired 3-diethylsulfamoylbenzoylaminobenzoic acids (**13a**, **13c**, **13d**, and **13e**) were then obtained by treating carboxylic acids **9**−**12** with thionyl chloride and catalytic DMF at reflux, followed by reaction with methyl anthranilate in pyridine and subsequent ester hydrolysis. Other activation-coupling strategies with these intermediates were unsuccessful and this efficient, albeit three-step, sequence became the standard procedure for making the amide bond of the benzoylaminobenzoic acid series. The phenylsulfonamide **13b** was obtained by Suzuki[17]-type palladium-mediated coupling between bromosulfonamide **13a** and phenylboronic acid. Using fluorosulfonamide **13e** as a common intermediate, alcohols and amines were used to readily displace the fluoro group via nucleophilic aromatic substitutions to provide compounds **13f**−**h**.

Using our standard procedure, 2-(3-phenoxybenzoylamino)benzoic acid (**15**) was synthesized from commercially available 3-phenoxybenzoic acid (Scheme 2). Originally, the synthesis of 2-(3-phenoxybenzoylamino)-benzoic acids with B ring para substitutions was accomplished by assembling the A and B rings, followed by reaction of the phenolate (generated in situ with NaH) with bromo benzene to install the C ring. Although operable, the yields were usually poor and the synthetic sequences were lengthy. Fortunately, developments in arylboronic acid coupling reactions allow the formation of diaryl ethers in high yields at room temperature through copper-catalyzed coupling of arylboronic acids and phenols.[18] Accordingly (Scheme 2), phenol **16** was brominated to provide the desired intermediate **18** as the major product after purification by flash column chromatography. Copper-catalyzed O-arylation of compounds **17** and **18** with phenylboronic acid proceeded smoothly with 1 equiv of $Cu(OAc)_2$ and excess base in CH_2Cl_2. Powdered 4 Å molecular sieves were added to the reaction mixture to quench any water generated during the reaction. After alkaline hydrolysis, compounds **19** and **20** underwent standard coupling

Scheme 2[a]

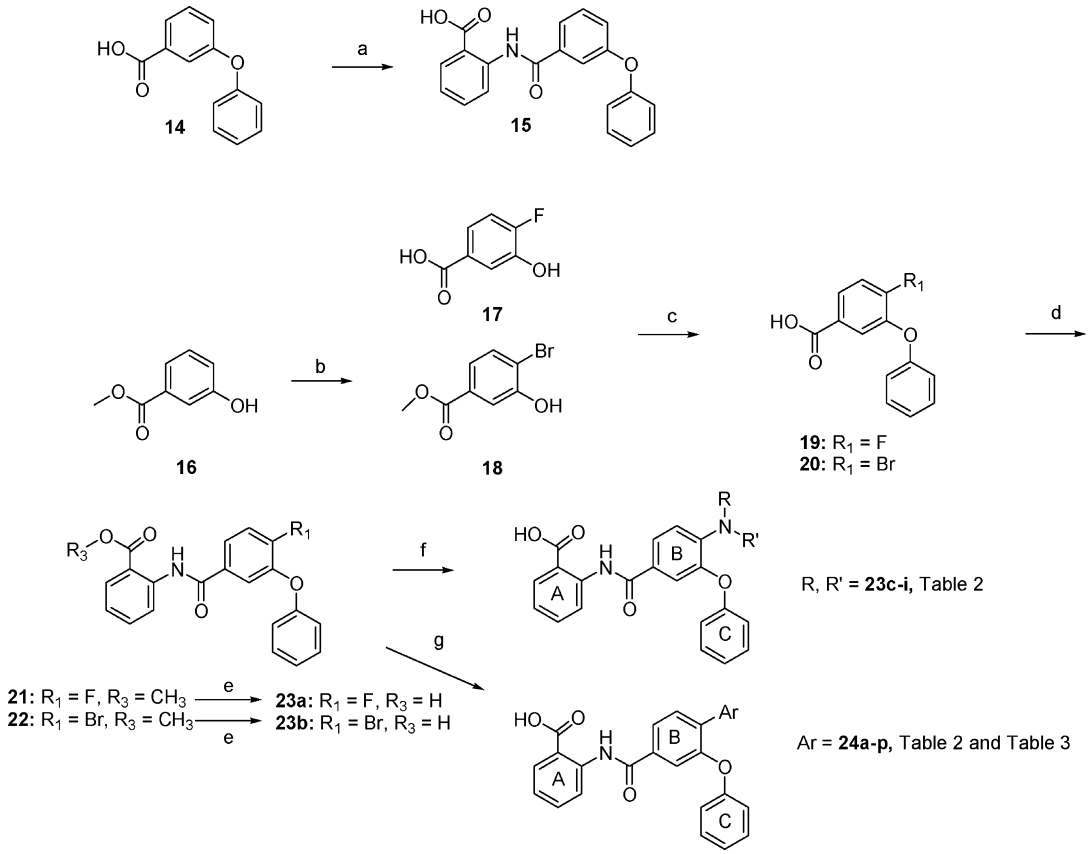

[a] Reagents: (a) (i) $SOCl_2$, DMF (cat.), reflux; (ii) methyl anthranilate, pyr; (iii) NaOH, THF/MeOH; (b) Br_2, HOAc; (c) (i) $PhB(OH)_2$, $Cu(OAc)_2$, TEA, 4 Å sieves, CH_2Cl_2; (ii) NaOH, THF/MeOH; (d) (i) $SOCl_2$, DMF (cat.), reflux; (ii) methyl anthranilate, pyr; (e) NaOH, THF/MeOH; (f) (i) amines, DMSO, 120 °C; (ii) NaOH, THF/MeOH; (g) (i) $ArB(OR^3)_2$, $Pd(PPh_3)_4$, aq Na_2CO_3, DME, reflux; (ii) NaOH, THF/MeOH.

procedures to yield **21** and **22**. Using the fluoro- or bromobenzoylaminobenzoic acid derivative, the B ring 4-position could be substituted with secondary amines and aromatic rings, respectively. Due to the electron-donating *o*-phenoxy group, nucleophilic replacement of the fluoro group with amines was sluggish and required harsh conditions. Nevertheless, compounds **23c**−**i** were obtained from **21** by heating with an excess of amine in DMSO (120−140 °C). Aromatic substitutions were accomplished by palladium-mediated coupling of **22** with commercially available arylboronic acids or esters to yield compounds **24a**−**p**.

Derivatives having various A ring systems (compounds **28a**−**f**) were obtained via the standard procedure and the appropriate aromatic amines (Scheme 3). For C ring modification, the anion of methyl 3-hydroxybenzoate (**16**), generated with NaH (1 equiv) was heated with 4-chloropyridine in dry DMF, which after the saponification of the ester gave acid **25**. Coupling as described previously afforded 2-[3-(pyridin-4-yloxy)benzoylamino]benzoic acid (**28g**). Compounds **28h**−**j** were obtained by condensing the appropriate substituted sodium phenolate with aromatic bromide **27** in the presence of catalytic CuCl.

Compounds **31** and **33** were synthesized according to Scheme 4. Using the general procedure for amide coupling, **20** was treated with $SOCl_2$ followed by reacting with 2-amino-6-methoxybenzoic acid in pyridine. However, instead of giving the desired amide product directly, the benzooxazinone **29** was formed, which upon hydrolysis with LiOH provided **30**. Cleavage of the methyl ether group by boron tribromide gave compound **31**. Compound **33** was obtained by Suzuki coupling of **30** with phenyl boronic acid followed by demethylation.

Results and Discussion

Cocrystallization studies of the benzoylaminobenzoic acid series of compounds resulted in a 2.6 Å resolution cocrystal structure of **13a** bound to full length *E. faecalis* FabH. Key features observed for ligand binding include an ionic interaction between the negatively charged carboxylate oxygen of **13a** and the γ-NH of the protonated imidazole ring of His250 (Figure 2). Additionally, both carboxylate oxygens of **13a** are involved in hydrogen bonding to the side chain NH_2 of Asn280. Together, these interactions define the orientation of the inhibitor within the active site, thus serving as the inhibitor "anchor". The remainder of the molecule aligns along the active site in an extended conformation, making hydrophobic interactions with protein residues nearby. In particular, Phe312 makes van der Waals (VDW) interactions with the inhibitor A ring (distance 3.3 Å). The *p*-bromide occupies a hydrophobic pocket created by residues Trp38, Ile39, Ile45, Val160, and Leu161 (Figure 2C), while the diethyl-sulfonamide portion of the inhibitor is largely solvent exposed and surrounded by several arginine and lysine residues (Figure 2D).

On the basis of information derived from the cocrystal structure of **13a**, our initial focus was to explore the pocket opening accessed by the B ring para position.

Scheme 3[a]

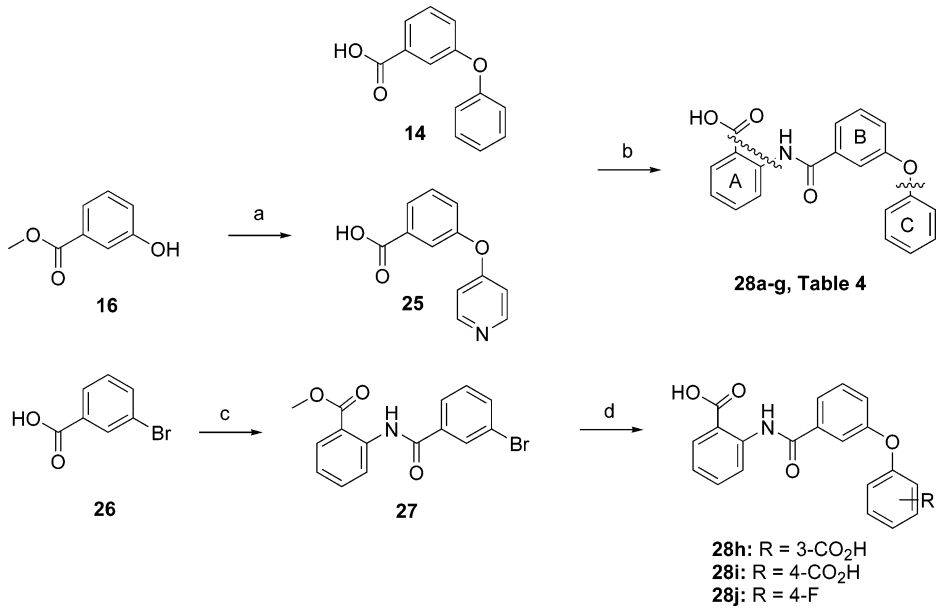

[a] Reagents: (a) NaH, CuCl, pyr/DMF, chloropyridine hydrochloride, 120 °C; (b) (i) $SOCl_2$, DMF (cat.), reflux; (ii) aromatic amines, pyr; (iii) hydrolysis: NaOH, THF/MeOH; or demethylation: BBr_3, CH_2Cl_2; (c) (i) $SOCl_2$, DMF (cat.), reflux; (ii) methyl anthranilate, pyr; (d) (i) phenols, NaH, CuCl, pyr, 120 °C; (ii) NaOH, THF/MeOH.

Scheme 4[a]

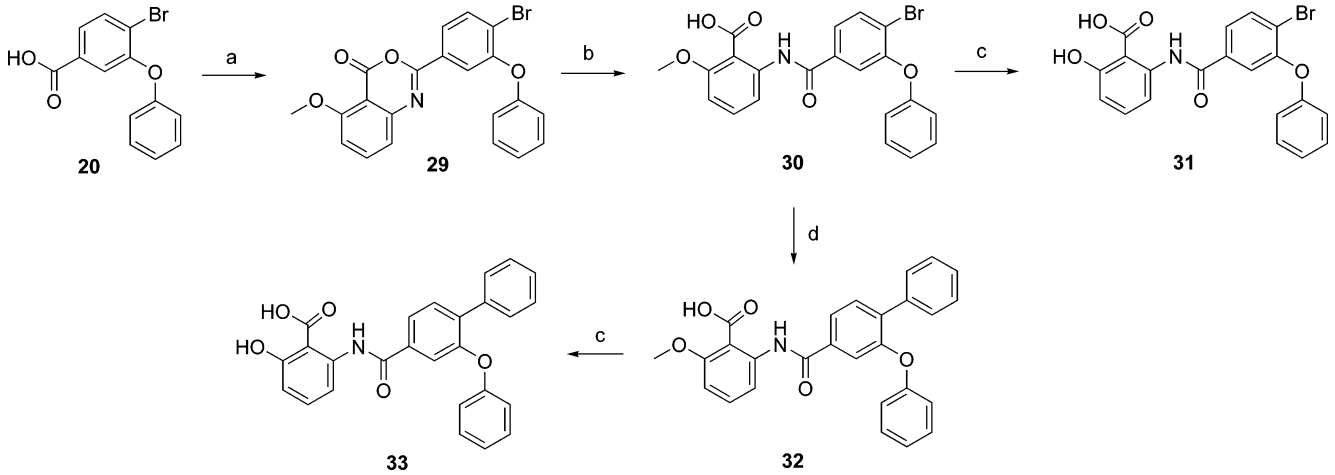

[a] Reagents: (a) (i) $SOCl_2$, DMF (cat.), reflux; (ii) 2-amino-6-methoxybenzoic acid, pyr; (b) LiOH, THF; (c) BBr_3, CH_2Cl_2; (d) $PhB(OH)_2$, $Pd(PPh_3)_4$, aq Na_2CO_3, DME, reflux.

Modeling studies predicted improved binding affinity by occupying the hydrophobic space and/or by forming π stacking interactions with surface Trp38. To explore this possibility, a set of para-substituted derivatives related to **13a** was synthesized. However, none of these derivatives showed better activity than the parent compound **13a** (Table 1).

A more in-depth conformational analysis suggests that the orientation of the sulfonamide group is influenced by these ortho substituents and as such disfavors the optimal conformation observed in the cocrystal structure. Clearly, combinations of the rather large and rigid sulfonamide group with ortho substituents would be problematic during optimization. These complications, along with the instability of the sulfonamide group to liver microsomes (data not shown), prompted the search for a suitable replacement. Modeling studies suggested that replacement of the sulfonamide with a phenoxy group might provide interaction with Phe224. To this end, compound **15** was synthesized and demonstrated similar activity (IC_{50} = 2.7 μM) against *E. faecalis* FabH, proved the principle of this design strategy.

Using compound **15** as our new lead, optimization of substituents on the B ring was pursued. The cocrystal structure of **13a** clearly indicated that the B ring and its amide bond needs to be coplanar, which obviates substitutions ortho to the amide. The meta carbon on the B ring is close to the side chain of Leu161 (4.2 Å); here even a small methyl group at this position resulted in a 100-fold loss in inhibition activity (**13c**, Table 1). The position para to the amide bond, however, offered a good vector toward an amphiphilic pocket formed by Trp38, Ile39, Ile45, Val160, and Leu161 at one side and Arg42 at the other side (Figure 2C). In a recently solved acetyl-CoA−FabH cocrystal structure (data not shown, but similar to the published *Escherichia coli* structure with CoA),[9] we observed that the size of this pocket had

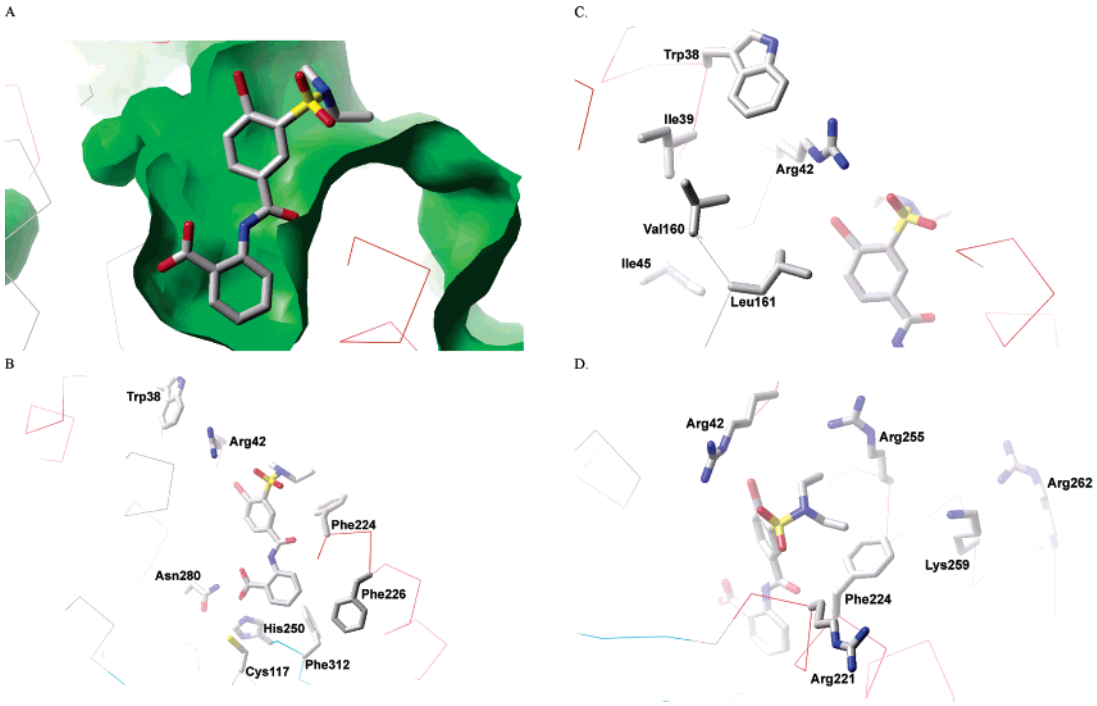

Figure 2. Compound **13a** (IC_{50} = 1.6 μM) bound in the active site of *E. faecalis* FabH. (A) Green molecular surface shows the active site cleft in which compound **13a** binds. (B) Details of protein−**13a** interactions. Key side chains lining the binding pocket are shown. The carboxylate of the compound **13a** makes hydrogen-bonding interactions with His250 and Asn280. (C) The bromine atom points toward a pocket lined with hydrophobic residues: Ile39, Ile45, Val160, and Leu161. (D) The sulfonamide group is located on the exposed face of the protein that is lined with basic residues.

Table 1. Diethylsulfonamide Derivatives as Inhibitors of FabH

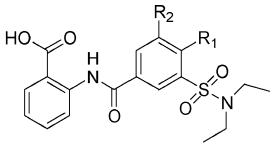

Compd	R_1	R_2	*E. fae* FabH IC_{50} (μM)
13a	Br	H	1.6
13b	Ph	H	1.6
13c	Br	Me	160
13d	OMe	H	11.4
13e	F	H	8.4
13f		H	2.2
13g	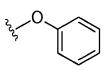	H	6.1
13h	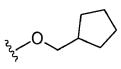	H	2.1

increased due to side chain movements of Trp38 and Arg42 likely induced by interaction of the CoA's adenine ring with the protein. This protein side chain mobility hampered our efforts to design a specific para functional group to fit into the binding pocket. Therefore, a more traditional approach was used to establish structure−activity relationships in this area. Using molecular modeling to exclude substituents that might insult highly conserved protein residues, a set of compounds (**23c**−**i**, **24a**−**c**, Table 2) with diverse rings at the 4-position was prepared. Replacement of the proton of **15** with a simple phenyl group (**24c**, Table 2) resulted in dramatic ca. 50-fold improvement in potency (IC_{50} = 2.7 μM vs 0.056 μM). Charged hydrophilic groups at the para position were not tolerated and resulted in significant decreases in potency (**23c**, **23d**, **23e**, and **24a**) (IC_{50} > 20 μM). Consistent with these results, the contour of an electrostatic map (ZAP, Tripos, Inc.) suggested that positively charged or partially positively charged groups in this pocket would be disfavored. Compounds with weakly basic groups at this position, such as **23h** and **23i**, showed 10-fold improved binding (IC_{50} = 0.29 and 0.27 μM, respectively). A complexed structure of **23i** with FabH (Figure 3) ultimately revealed the nature of the pocket and its interactions with para substituents. The dimethylpiperidine ring establishes hydrophobic interactions with the adjacent protein side chains and accounts for the observed 10-fold improvement in potency. The 50-fold improvement observed for compound **24c** is likely due to a combination of factors: (1) the phenyl group occupies this hydrophobic space; (2) it also forms stacking interactions with the indole ring of Trp38; (3) intramolecular stacking interactions between the two adjacent aromatic rings on the B ring conformationally preorganized the two rings, leading to favorable interactions with the protein active site.

Encouraged by the **24c** result, a series of compounds with different substitutions on the distal arene (Table 3) was synthesized. Most of these compounds show submicromolar IC_{50} values, the best one being **24i** (IC_{50} = 28 nM). One possible explanation for the rather flat SAR in this region is that the stronger stacking interaction

Table 2. [3-Phenoxybenzoylamino]benzoic Acid Derivatives as Inhibitors of FabH: Para-Substitutions on the B Ring

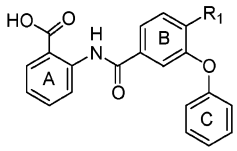

Compd	R_1	*E. fae* FabH IC_{50} (μM)
15	H	2.7
23a	F	3.8
23b	Br	1.1
23c	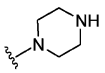	185
23d	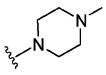	25
23e	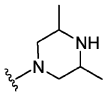	38
23f		3.2
23g		1.2
23h		0.29
23i	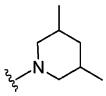	0.27
24a		22
24b		0.11
24c		0.056

resulted in organization of the flexible region around Trp38; thus, the entropic energy cost may cancel out any stacking energy gain. This rationale is supported by the crystal structures of **13a** and **23i** (Figure 4), which when overlayed reveals the changes in side chain conformation by Arg42 and Trp38, although the main chain is essentially invariant. FabH cocrystal structures from this series (**24a**–**p**) are awaited to confirm the hypothesis.

Concurrent with exploration of the hydrophobic pocket occupied by the para-position substituent of the B ring was the optimization of the A and C rings (Table 4).

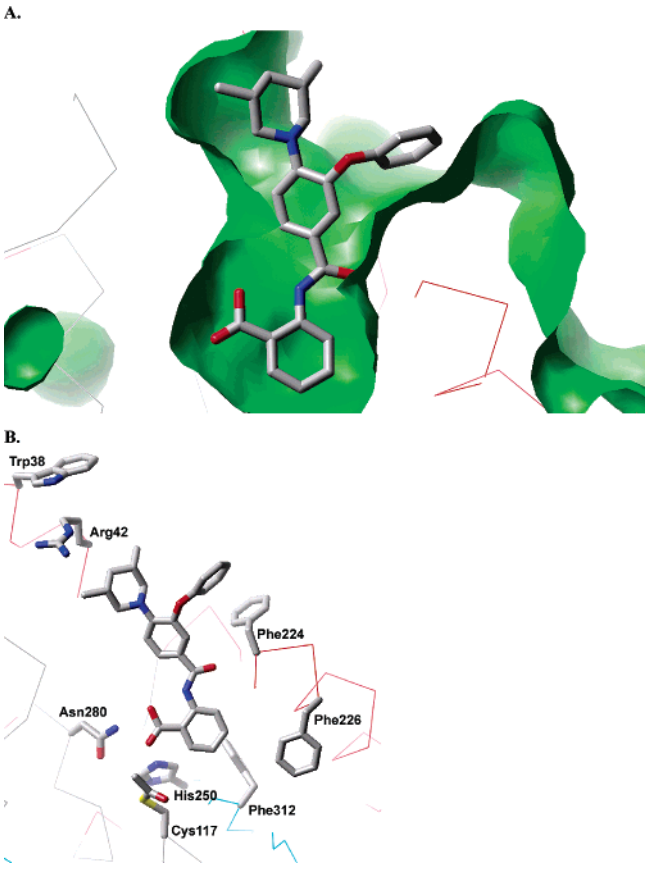

Figure 3. Compound **23i** (IC_{50} = 0.27 μM) bound in the active site of *E. faecalis* FabH. (A) Green molecular surface shows the active site cleft in which compound **23i** binds. (B) Details of protein–**23i** interactions. Key side chains lining the binding pocket are shown. The Cys117 side chain is found to be acetylated in this crystal structure.

Table 3. Aromatic Substitutions on the Para Position of [3-Phenoxybenzoylamino]benzoic Acid Derivatives

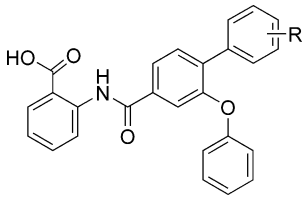

compd	R	*E. faecalis* FabH IC_{50} (μM)	compd	R	*E. faecalis* FabH IC_{50} (μM)
24c	H	0.056	24j	3-iPr	0.79
24d	4-CF_3	0.096	24k	3-OCF_3	0.47
24e	4-Me	0.16	24l	3-Me-4-F	0.24
24f	4-CO_2H	2.1	24m	3-Cl-4-F	0.57
24g	4-OH	0.41	24n	3,4-di-F	0.33
24h	4-OEt	0.22	24o	3-Me-4-Cl	0.25
24i	4-SO_2Me	0.028	24p	2,4-di-F	0.16

The A ring is located deep in the active site pocket and is oriented to provide optimal ionic interactions between the ligand COO^- and the protonated imidazole side chain of His250. Intramolecular neutralization of the carboxylate group by changing the benzene ring to a pyridine ring (**28c** and **28d**) diminishes the inhibition activity. Additionally, a thiophene ring at this position did not improve the inhibitor potency (**28a** and **28b**) either. In addition to the interaction between the aromatic COOH and the protein residues, the aromatic

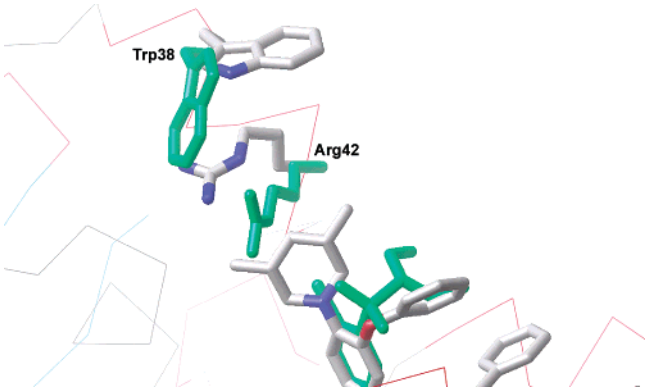

Figure 4. Flexibility of the side chains on the protein surface. Trp38 and Arg42 side chains adopt different conformations in the **23i** bound structure (shown in atom colors) as compared with **13a** bound structure (shown in monochrome green).

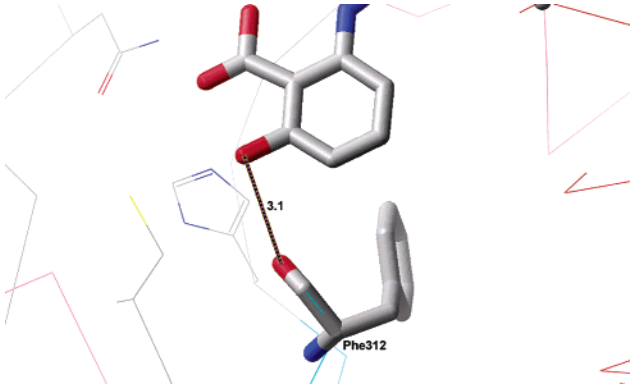

Figure 5. Model of compound **28f** bound to *E. faecalis* FabH. The interaction between the hydroxyl group and the carbonyl oxygen of Phe312 is likely responsible for the 7-fold improvement in the binding affinity.

Table 4. [3-Phenoxybenzoylamino]benzoic Acid Derivatives as Inhibitors of FabH: Modifications of Ring A and C

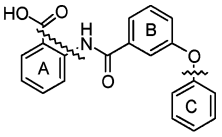

Compd	"A"	"C"	*E. fae* FabH IC_{50} (μM)
15	Ph	Ph	2.7
28a		Ph	10.1
28b		Ph	43.0
28c		Ph	290
28d		Ph	> 1000
28e	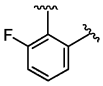	Ph	6.0
28f	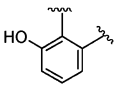	Ph	0.41
28g	Ph	4-Pyr	10
28h	Ph	3-CO_2H-Ph	3.7
28i	Ph	4-CO_2H-Ph	4.4
28j	Ph	4-F-Ph	5.0

ring is also surrounded by a tight array of hydrophobic residues including Leu194, Ile223, Phe226, Ala227, Ala252, and Phe312. Whether any substitution ortho to the COOH on the benzene ring would be tolerated

Table 5. Potent Inhibitors of FabH: Effect of Adding OH Ortho to the Carboxylic Acid

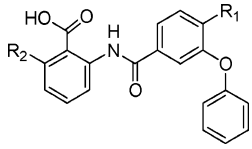

compd	R_1	R_2	*E. faecalis* FabH IC_{50} (μM)	compd	R_1	R_2	*E. faecalis* FabH IC_{50} (μM)
15	H	H	2.7	28f	H	OH	0.41
23b	Br	H	1.1	31	Br	OH	0.062
24c	Ph	H	0.056	33	Ph	OH	0.004

remained an open question. Models based on the cocrystal structure of **23i** suggested that an *o*-OH group would be positioned to form a 3.1 Å hydrogen-bonding interaction with the backbone carbonyl of Phe312 (Figure 5). To test this theory, compound **28f** (IC_{50} = 0.41 μM) was made and indeed showed improved binding (~7-fold) as compared to nonhydroxylated compound **15** (IC_{50} = 2.7 μM). The same trend was observed upon comparison of **23b** with **31** (IC_{50} = 1.1 and 0.062 μM) and **24c** with **33** (IC_{50} = 0.056 and 0.004 μM), as shown in Table 5. Adding an *o*-OH does provide additional potency, which makes compound **33** the most potent compound in the series so far.

Ring C of the inhibitors is located on the surface of the active site. Besides a few flexible arginine residues, there is a phenylalanine residue (Phe224). Compounds **28g**–**j** were synthesized with the aim to accomplish one or both of the following objectives: (1) to strengthen π–π stacking interaction and (2) to form ionic interactions with positively charged surface arginine residues. However, none of these compounds showed improved binding. Analysis from the cocrystal structure of compound **23i** and the enzyme (Figure 2) suggested that the relative positioning of the benzene C ring to arene of Phe224 does not provide an optimal π–π stacking interaction. Interactions with solvent-exposed arginines do not provide further improvement in binding affinity.

To generate data concerning the broad spectrum potential of these compounds, the IC_{50} values of selected compounds against FabH enzymes from different pathogens were determined (Table 6). Although this series is highly potent against *E. faecalis* and *Streptococcus pyogenes* FabH (IC_{50} < 100 nM), they only show moder-

Table 6. Cross-Genus Inhibitor Activity

	IC_{50} (μM)			
compd	E. faecalis	S. pyogenes	S. aureus	H. influenzae
24c	0.056	0.05	10	> 100
24i	0.028	0.003	24	> 100
31	0.062	0.034	12.3	20
33	0.004	0.004	3.8	2.4

Table 7. Minimum Inhibitory Concentrations (MIC) for Select Benzoylaminobenzoic Acid FabH Inhibitors[a]

	MIC (μg/mL)					
compd	Sa	Spn	Spy	Ef	Nm	Ec
23i	5.6	2.8	2.8	11.3	2.8	5.6
24c	11.3	1.4	ND	22	1.4	1.4
24d	5.6	0.7	2.8	5.6	1.4	0.7
24i	45	45	22	>45	5.6	5.6
24j	5.6	1.4	2.8	5.6	1.4	2.8
24l	5.6	0.7	2.8	2.8	0.7	0.7
24o	5.6	2.8	1.4	5.6	0.7	0.7
24p	5.6	2.8	2.8	11.3	0.36	0.7
31	45	45	11.3	>45	2.8	2.8
33	22	22	5.6	>45	1.4	1.4

[a] Sa = *S. aureus* MRSA 703; Spn = *S. pneumoniae* ATCC 6301; Spy = *S. pyogenes* NZ131; Ef = *E. faecalis* VRE 583; Nm = *Neisseria meningitides* MC58 (+PMB); Ec = *E. coli* TolC− (+PMB).

ate activity (IC_{50} = 4−24 μM) against *Staphylococcus aureus* and essentially lack significant activity against *H. influenzae* FabH (IC_{50} = 2.5→100 μM). Clearly there is a structural difference in the active sites of these latter proteins that amino acid sequence conservation and alignments are not revealing. To provide this important data, crystal structures were solved for *S. aureus* and *H. influenzae* proteins both with and without bound inhibitor.[19] These structures provided significant insight into the structural differences, and structure-based optimization of the compounds in the series with broad-spectrum FabH inhibition is in progress.

Antibacterial Activity. Determination of minimum inhibitory concentrations (MIC) for several Gram-positive and -negative pathogenic bacteria showed that most of the potent enzyme inhibitors also possessed modest to strong antibacterial activity against both Gram-positive and -negative bacterium (Table 7). However, poor activity was observed for several compounds that are potent inhibitors of the enzyme in vitro (**24i**, **31**, and **33**). These results suggest that these compounds either fail to penetrate the bacterial cell membranes or are actively pumped out of the bacterial cells by efflux pumps. These hypotheses are supported by observed activity, albeit modest, against the *E. coli* TolC− mutant in the presence of the membrane permeablizing agent polymyxin B.

Conclusion

FabH is an emerging target for the development of novel antibacterial chemotherapeutics. Structure-based design of a series of benzoylaminobenzoic acid derivatives led to the discovery of potent inhibitors of type II fatty acid synthase III (FabH). These FabH inhibitors demonstrated potent antibacterial activity (MIC) and as such have the potential to be novel and potent antibacterial agents. Given the unforeseen structural differences within the active site of some pathogenic FabH enzymes, the key to discovering inhibitors with broad-spectrum antibacterial activity lies in a detailed understanding of the FabH active sites. Toward this end, new structural data is guiding further modifications of the current series with the hopes of improving both enzymatic inhibition and physical properties.

Experimental Section

General Chemistry Methods. Proton NMR spectra were collected at 300 MHz on a Bruker Avance 300 spectrometer, and chemical shifts are reported in parts per million (δ) downfield from tetramethylsilane as internal standard. Atmospheric pressure ionization electrospray mass spectra and LCMS were recorded on an Agilent 1100 Series LC/MSD-SL 1946D spectrometer equipped with an Agilent 100 series HPLC system. Silica gel 60 (230−400 mesh) from EM Science was used for column chromatography, and analytical or preparative thin-layer chromatography was conducted using EM Science Kieselgel 60 F_{254} plates. An Agilent 1100 Series HPLC with an Agilent Zorbax Eclipse XDB-C8 (4.6 × 150 mm) reversed phase column was used for analytical HPLC analyses. Preparative RP-HPLC was performed on a Gilson instrument with a MetaSil AQ 10 μm C18 column. The elution buffer was an A/B gradient, where A = H_2O−0.1% TFA and B = ACN−0.1% TFA. For reactions performed under anhydrous conditions, glassware was either oven- or flame-dried and the reaction was run under a positive pressure of nitrogen. Anhydrous solvents were used as purchased from commercial sources. Except where noted, reagents were purchased from commercial sources and used without further purification. The reported yields are the actual isolated yields of purified material and are not optimized.

4-Bromo-3-diethylsulfamoylbenzoic Acid (9). Representative Procedure for 9−12. A mixture of 4-bromobenzoyl chloride (**1**, 1 g, 4.56 mmol) in chlorosulfonic acid (3 mL) was heated to 140 °C for 4 h, after which time HPLC indicated complete conversion of the starting material to the intermediate, 4-bromo-3-chlorosulfonylbenzoic acid (**5**). The reaction mixture was slowly dripped over ice and filtered. The solid was dried in vacuo to yield the intermediate (**5**, 954 mg, 70%), which was carried forward without further purification. 4-Bromo-3-chlorosulfonylbenzoic acid (**5**, 954 mg, 3.18 mmol) was dissolved in EtOAc (20 mL), and diethylamine (0.99 mL, 9.54 mmol) was then added. After stirring at room temperature for 24 h, the reaction mixture was concentrated. The resulting residue was dissolved in H_2O and extracted with EtOAc and 3 N HCl. The combined organic layers were dried over anhydrous $MgSO_4$ and concentrated in vacuo to yield the 4-bromodiethylsulfamoylbenzoic acid intermediate (**9**, 413 mg, 39%).

4-Bromo-3-diethylsulfamoyl-5-methylbenzoic acid (10): ^{1}H NMR (DMSO-d_6) δ 13.62 (br s, 1H), 8.36 (d, J = 2.0 Hz, 1H), 8.16 (d, J = 2.0 Hz, 1H), 4.07 (q, 4H), 2.53 (s, 3H), 1.11 (t, 6H); LCMS (API-ES) *m/z* 349.9, 351.9 [M + H^+]; 347.9, 349.9 [M + H^-].

3-Diethylsulfamoyl-4-methoxybenzoic acid (11): ^{1}H NMR (DMSO-d_6) δ 13.14 (br s, 1H), 8.36 (d, J = 2.2 Hz, 1H), 8.18 (dd, J = 2.2 and 8.7 Hz, 1H), 7.37 (d, J = 8.7 Hz, 1H), 4.01 (s, 3H), 3.27 (q, 4H), 1.04 (t, 6H); LCMS (API-ES) *m/z* 288.0 [M + H^+].

3-Diethylsulfamoyl-4-fluorobenzoic acid (12): ^{1}H NMR (DMSO-d_6) δ 13.55 (br s, 1H), 8.30 (m, 1H), 7.76 (m, 1H), 7.64 (m, 1H), 3.35 (q, 4H), 1.10 (t, 6H); LCMS (API-ES) *m/z* 276.0 [M + H^+]; 274.0 [M + H^-].

General Procedure for Amide Bond Formation of Substituted Benzoylaminobenzoic Acid Derivatives. The acid (1.5 equiv) was converted to the acid chloride by refluxing in thionyl chloride with a catalytic amount of DMF. After 2−4 h, the reaction mixture was concentrated and suspended in pyridine. The mixture was cooled to 0 °C under N_2, and methyl anthranilate (1 equiv) was added. After stirring for 24 h at room temperature, the reaction mixture was concentrated, neutralized with 1 N HCl, and extracted with EtOAc (3×). The organics were washed with brine, dried over anhydrous

$MgSO_4$, and concentrated in vacuo. The methyl ester was then hydrolyzed with 1 N NaOH in THF/MeOH (2:1). The final compound was purified using RP-HPLC.

2-[(2-Diethylsulfamoyl-biphenyl-4-carbonyl)amino]benzoic Acid (13b). A solution of 2-(4-bromo-3-diethylsulfamoylbenzoylamino)benzoic acid methyl ester (**13a**, 40 mg, 0.098 mmol), phenylboronic acid (13.1 mg, 0.108 mmol), $Pd(PPh_3)_4$ (6 mg, 0.005 mmol), and 2 M Na_2CO_3 (0.147 mL, 0.294 mmol) in DME (3 mL) was refluxed under N_2 for 24 h. Upon cooling the reaction to room temperature, it was diluted with EtOAc and washed with brine and water, dried over anhydrous $MgSO_4$, and concentrated in vacuo. The methyl ester was then hydrolyzed, and the crude material was acidified with 1 N HCl and purified using RP-HPLC to afford the final compound **13b** (12 mg, 27%): ^{1}H NMR (300 MHz, DMSO-d_6) δ 13.95 (br s, 1H), 12.40 (s, 1H), 8.74 (d, J = 8.4 Hz, 1H), 8.60 (s, 1H), 8.25 (d, J = 7.9 Hz, 1H), 8.12 (d, J = 7.9 Hz, 1H), 7.75 (t, J = 7.7 Hz, 1H), 7.62 (d, J = 6.4 Hz, 1H), 7.45 (m, 5H), 7.30 (t, J = 7.3 Hz, 1H), 2.84 (q, J = 6.9 Hz, 4H), 0.94 (t, J = 7.1 Hz, 6H); LCMS (API-ES) *m/z* 453.0 [M + H$^+$]; 451.0 [M + H$^-$].

2-(4-Bromo-3-diethylsulfamoyl-5-methylbenzoylamino)-benzoic acid (13c) was prepared according to the general procedure for amide bond formation: ^{1}H NMR (300 MHz, DMSO-d_6) δ 13.95 (br s, 1H), 12.35 (s, 1H), 8.67 (d, J = 8.1 Hz, 1H), 8.42 (s, 1H), 8.20 (s, 1H), 8.10 (d, J = 8.0 Hz, 1H), 7.71 (m, 1H), 7.27 (m, 1H), 3.51 (q, J = 6.9 Hz, 4H), 2.59 (s, 3H), 1.12 (t, J = 7.0 Hz, 6H); LCMS (API-ES) *m/z* 470.8 [M + H$^+$]; 467.9 [M + H$^-$].

2-(3-Diethylsulfamoyl-4-methoxybenzoylamino)benzoic acid (13d) was prepared according to the general procedure for amide bond formation: ^{1}H NMR (300 MHz, DMSO-d_6) δ 14.05 (br s, 1H), 12.31 (s, 1H), 8.72 (d, J = 8.0 Hz, 1H), 8.45 (d, J = 2.3 Hz, 1H), 8.22 (dd, J = 2.4 and 8.7 Hz, 1H), 8.09 (dd, J = 1.5 and 7.9 Hz, 1H), 7.71 (t, J = 7.1 Hz, 1H), 7.49 (d, J = 8.8 Hz, 1H), 7.26 (t, J = 8.1 Hz, 1H), 4.04 (s, 3H), 3.31 (q, J = 7.0 Hz, 4H), 1.07 (t, J = 7.1 Hz, 6H); LCMS (API-ES) *m/z* 407.0 [M + H$^+$]; 405.0 [M + H$^-$].

2-(3-Diethylsulfamoyl-4-fluorobenzoylamino)benzoic acid (13e) was prepared according to the general procedure for amide bond formation: ^{1}H NMR (300 MHz, DMSO-d_6) δ 13.95 (br s, 1H), 12.29 (s, 1H), 8.65 (d, J = 7.7 Hz, 1H), 8.43 (dd, J = 2.4 and 6.7 Hz, 1H), 8.31 (m, 1H), 8.09 (dd, J = 1.5 and 7.9 Hz, 1H), 7.76 (m, 2H), 7.31 (t, J = 7.9 Hz, 1H), 3.33 (q, J = 7.0 Hz, H), 1.12 (t, J = 7.1 Hz, 6H); LCMS (API-ES) *m/z* 395.0 [M + H$^+$]; 393.0 [M + H$^-$].

2-(3-Diethylsulfamoyl-4-piperidin-1-ylbenzoylamino)-benzoic Acid (13f). To a stirred solution of 2-(3-diethylsulfamoyl-4-fluorobenzoylamino)benzoic acid (**13e**, 30 mg, 0.07 mmol) and piperidine (0.015 mL, 0.15 mmol) in DMF was added potassium carbonate (28 mg, 0.2 mmol). The reaction mixture was allowed to heat at 130 °C for 24 h. The reaction mixture was cooled; diluted with EtOAc, H_2O, and 1 N HCl; and extracted with EtOAc (2×). Combined organic layers were washed with brine and H_2O, dried over anhydrous $MgSO_4$, and concentrated in vacuo. The crude material was purified using RP-HPLC to afford the final compound **13f** (25 mg, 78%): ^{1}H NMR (300 MHz, DMSO-d_6) δ 13.95 (br s, 1H) 12.29 (s, 1 H), 8.72 (d, J = 7.8 Hz, 1H), 8.50 (d, J = 2.2 Hz, 1H), 8.16 (dd, J = 2.2 and 8.4 Hz, 1H), 8.09 (dd, J = 1.5 and 7.9 Hz, 1H), 7.71 (t, 1H), 7.64 (d, J = 8.4 Hz, 1H), 7.26 (t, J = 7.9 Hz, 1H), 3.35 (q, J = 7.1 Hz, 4H), 3.00 (m, 4H), 1.60 (m, 6H), 1.00 (t, J = 7.1 Hz, 3H); LCMS (API-ES) *m/z* 460.0 [M + H$^+$]; 458.0 [M + H$^-$].

2-(3-Diethylsulfamoyl-4-phenoxybenzoylamino)benzoic Acid (13g). To a stirred solution of phenol (14 mg, 0.15 mmol) in anhydrous DMF was added NaH (60%, 8 mg, 0.2 mmol). The reaction mixture was stirred at room temperature for 0.5 h and then 2-(3-diethylsulfamoyl-4-fluorobenzoylamino)benzoic acid methyl ester (30 mg, 0.07 mmol) was added. The reaction mixture was allowed to heat at 120 °C for 24 h. The reaction mixture was cooled; diluted with EtOAc, H_2O, and 1 N HCl; and extracted with EtOAc (2×). Combined organic layers were washed with brine and H_2O, dried over anhydrous $MgSO_4$, and concentrated in vacuo. The crude material was purified using RP-HPLC to afford the final compound **13g** (15 mg, 46%): ^{1}H NMR (300 MHz, DMSO-d_6) δ 13.95 (br s, 1H) 12.29 (s, 1 H), 8.69 (d, J = 7.7 Hz, 1H), 8.55 (d, J = 2.3 Hz, 1H), 8.17 (dd, J = 2.3 and 8.7 Hz, 1H), 8.09 (dd, J = 1.5 and 7.9 Hz, 1H), 7.72 (t, J = 8.1 Hz, 1H), 7.56 (m, 2H), 7.10−7.38 (m, 5H), 3.35 (q, J = 7.1 Hz, 4H), 1.12 (t, J = 7.1 Hz, 3H); LCMS (API-ES) *m/z* 469.0 [M + H$^+$]; 467.0 [M + H$^-$].

2-(4-Cyclopentylmethoxy-3-diethylsulfamoylbenzoylamino)benzoic Acid (13h). To a stirred solution of 2-(3-diethylsulfamoyl-4-fluorobenzoylamino)benzoic acid (**13e**, 30 mg, 0.076 mmol) and cyclopentane−methanol (1 mL, 0.924 mmol) was added potassium carbonate (32 mg, 0.228 mmol). The reaction mixture was allowed to heat at 135 °C for 24 h. After confirming the product by LCMS, the reaction mixture was cooled; diluted with EtOAc, H_2O, and 1 N HCl; and extracted with EtOAc (2×). Combined organic layers were washed with brine and H_2O, dried over anhydrous $MgSO_4$, and concentrated in vacuo. The crude material was purified using RP-HPLC to afford the final compound **13h** (12.1 mg, 34%): ^{1}H NMR (300 MHz, DMSO-d_6) δ 12.32 (s, 1H), 8.72 (d, J = 8.3 Hz, 1H), 8.46 (d, J = 2.3 Hz, 1H), 8.19 (dd, J = 2.3, 8.7 Hz, 1H), 8.09 (dd, J = 1.4 and 7.9 Hz, 1H), 7.70 (dt, J = 1.5 and 7.8 Hz, 1H), 7.48 (d, J = 8.8 Hz, 1H), 7.25 (t, J = 7.9 Hz, 1H), 4.13 (d, J = 7.2 Hz, 2H), 2.54 (overlap with DMSO, 4H), 1.86 (m, 1H), 1.63 (m, 4H), 1.43 (m, 1H), 1.28 (m, 1H), 1.07 (t, J = 7.1 Hz, 6H), 0.90 (m, 1H); LCMS (API-ES) *m/z* 475.0 [M + H$^+$]; 473.0 [M + H$^-$].

2-(3-Phenoxybenzoylamino)benzoic acid (15) was prepared according to the general procedure for amide bond formation: ^{1}H NMR (300 MHz, DMSO-d_6) δ 12.28 (s, 1H), 8.69 (d, J = 8.3 Hz, 1H), 8.08 (d, J = 7.9 Hz, 1H), 7.74 (t, J = 7.4 Hz, 1H), 7.68 (d, J = 4.7 Hz, 1H), 7.64 (d, J = 7.7 Hz, 1H), 7.57 (s, 1H), 7.48 (t, J = 7.8 Hz, 2H), 7.32 (dd, J = 2.4, 7.8 Hz, 1H), 7.25 (t, J = 7.4 Hz, 2H), 7.14 (d, J = 8.5 Hz, 2H); LCMS (API-ES) *m/z* 334.0 [M + H$^+$]; 332.0 [M + H$^-$].

Methyl 4-Bromo-3-hydroxybenzoate (18). To methyl 3-hydroxybenzoate (**16**, 10 g, 66 mmol) in acetic acid (40 mL) was added bromine (3.4 mL, 66 mmol) dropwise. After stirring at room temperature for 4 h, the reaction mixture was diluted with water and extracted three times with EtOAc. Organics were dried over anhydrous $MgSO_4$. Purification by flash column chromatography (10% EtOAc/hexane) provided **18** as a white solid (6.8 g, 44%): ^{1}H NMR (300 MHz, DMSO-d_6) δ 10.78 (s, 1H), 7.67 (d, J = 8.2 Hz, 1H), 7.56 (d, J = 2.0 Hz, 1H), 7.33 (dd, J = 2.0 and 8.2 Hz, 1H), 3.86 (s, 3H); LCMS (API-ES) *m/z* 228.9, 230.9 [M + H$^-$].

4-Fluoro-3-phenoxybenzoic Acid (19). A mixture of 4-fluoro-3-hydroxybenzoic acid (**17**, 641 mg, 4.0 mmol), phenylboronic acid (975 mg, 8 mmol), copper acetate (726.6 mg, 4 mmol), TEA (2.78 mL, 20 mmol), and 4 Å molecular sieves in DCM (40 mL) was stirred at room temperature for 2 days. Once the reaction was complete, the reaction mixture was filtered and the filtrate concentrated in vacuo. The resulting residue was diluted with EtOAc and acidified with 1 N HCl. The aqueous layer was extracted two times with EtOAc, and the organics were washed with brine, dried over anhydrous $MgSO_4$, and concentrated in vacuo. Purification by flash column chromatography (20% hexane/EtOAc with 0.1% MeOH) provided the acid (**19**, 300 mg, 32%): ^{1}H NMR (300 MHz, DMSO-d_6) δ 7.77 (m, 1H), 7.61 (d, J = 8.4 Hz, 1H), 7.39 (m, 3H), 7.20 (t, J = 6.6 Hz, 1H), 7.04 (d, J = 8.0 Hz, 2H); LCMS (API-ES) *m/z* 231.1 [M + H$^-$].

4-Bromo-3-phenoxybenzoic Acid (20). A mixture of 4-bromo-3-hydroxybenzoic acid methyl ester (**18**, 2.1 g, 9.1 mmol), phenyl boronic acid (2.2 g, 18 mmol), copper acetate (1.65 g, 9.1 mmol), TEA (6.26 mL, 45 mmol), and 4 Å molecular sieves in DCM (100 mL) was stirred at room temperature for 20 h. Once the reaction was complete, the reaction mixture was filtered and the filtrate concentrated in vacuo. The resulting residue was diluted with EtOAc and saturated $NaHCO_3$. The aqueous layer was extracted twice with EtOAc, and the organics were washed with brine, dried over anhydrous $MgSO_4$, and concentrated in vacuo. Purification by flash column chromatography (12.5% EtOAc/hexane) gave the in-

termediate, 4-bromo-3-phenoxybenzoic acid methyl ester (1.26 g), which was then hydrolyzed using 1 N NaOH (10.28 mL, 10.28 mmol) and THF/MeOH (25 mL/12.5 mL) to provide the acid (**20**, 1.08 g, 40% in two steps): ^{1}H NMR (300 MHz, DMSO-d_6) δ 13.39 (s, 1H), 7.91 (d, J = 8.3 Hz, 1H), 7.67 (dd, J = 1.9 and 8.3 Hz, 1H), 7.47 (m, 2H), 7.42 (d, J = 1.9 Hz, 1H), 7.26 (m, 1H), 7.08 (m, 2H); LCMS (API-ES) *m/z* 290.9, 292.9 [M + H$^-$].

2-(4-Fluoro-3-phenoxybenzoylamino)benzoic Acid Methyl Ester (21). Using the general procedure for making amide, the acid (**19**, 600 mg, 3 mmol) was first converted to the acid chloride and then reacted with methyl anthranilate (0.389 mL, 3 mmol). The crude material was purified by flash column chromatography (5−10% EtOAc/hexane) to yield **21** (420 mg, 38%): ^{1}H NMR (300 MHz, DMSO-d_6) δ 11.51 (s, 1H), 8.43 (d, J = 7.7 Hz, 1H), 8.02 (dd, J = 1.5 and 7.9 Hz, 1H), 8.01 (m, 1H), 7.66−7.73 (m, 3H), 7.48 (m, 2H), 7.29 (m, 2H), 7.14 (d, J = 7.8 Hz, 2H), 3.88 (s, 3H); LCMS (API-ES) *m/z* 366.0 [M + H$^+$].

2-(4-Bromo-3-phenoxybenzoylamino)benzoic Acid Methyl Ester (22). Using the general procedure for making amide, the acid (**20**, 1.08 g, 3.67 mmol) was first converted to the acid chloride and then reacted with methyl anthranilate (0.347 mL, 2.68 mmol). The crude material was purified by flash column chromatography (6.25−12.5% EtOAc/hexane) to yield **22** (1.12 g, 98%): ^{1}H NMR (300 MHz, DMSO-d_6) δ 11.53 (s, 1H), 8.44 (d, J = 8.0 Hz, 1H), 7.98−8.04 (m, 2H), 7.66−7.72 (m, 2H), 7.47−7.54 (m, 3H), 7.24−7.30 (m, 2H), 7.10−7.13 (m, 2H), 3.85 (s, 3H); LCMS (API-ES) *m/z* 425.9, 427.9 [M + H$^+$]; 425.9 [M + H$^-$].

2-(4-Fluoro-3-phenoxybenzoylamino)benzoic Acid (23a). The ester (**21**) was saponified using 1 N NaOH in THF/MeOH to provide the acid (**23a**): ^{1}H NMR (300 MHz, DMSO-d_6) δ 12.17 (s, 1H), 8.62 (d, J = 8.3 Hz, 1H), 8.07 (dd, J = 1.5 and 7.9 Hz, 1H), 7.83 (m, 1H), 7.66−7.72 (m, 3H), 7.47 (m, 2H), 7.25 (m, 2H), 7.12 (d, 2H); LCMS (API-ES) *m/z* 352.0 [M + H$^+$]; 350.0 [M + H$^-$].

2-(4-Bromo-3-phenoxybenzoylamino)benzoic Acid (23b). The ester (**22**) was saponified using 1 N NaOH in THF/MeOH to provide the acid (**23b**): ^{1}H NMR (300 MHz, DMSO-d_6) δ 12.19 (s, 1H), 8.60 (d, J = 7.6 Hz, 1H), 8.06 (m, 2H), 7.71 (m, 2H), 7.56 (s, 1H), 7.45 (m, 2H), 7.24 (m, 2H), 7.10 (m, 2H); LCMS (API-ES) *m/z* 409.9, 411.8 [M + H$^-$].

General Procedure for Replacement of Fluoro Group with Amines To Make Derivatives 23c−i. A mixture of 2-(4-fluoro-3-phenoxybenzoylamino)benzoic acid methyl ester (**21**, 1 equiv) and the amine (5 equiv) was heated at 120 °C in a scintillation vial with DMSO (1 mL) for a few days. After that the reaction mixture was diluted with H_2O and EtOAc. Brine was used to help separate the layers. The combined organics were dried over anhydrous $MgSO_4$ and concentrated in vacuo. The ester was then saponified using 1 N NaOH in THF/MeOH and purified using RP-HPLC to afford the final compound.

2-(3-Phenoxy-4-piperazin-1-ylbenzoylamino)benzoic acid (23c) was prepared according to the general procedure for replacement of fluoro group: ^{1}H NMR (300 MHz, DMSO-d_6) δ 8.67 (d, J = 7.4 Hz, 1H), 8.07 (d, J = 8.1 Hz, 1H), 7.53 (d, J = 8.6 Hz, 1H), 7.42 (m, 1H), 7.42 (m, 3H), 7.33 (d, J = 8.3 Hz, 1H), 7.20 (t, J = 7.3 Hz, 2H), 7.04 (d, J = 8.4 Hz, 2H), 3.53 (m, 2H), 3.11 (m, 2H), 2.62 (m, 4H); LCMS (API-ES) *m/z* 418.0 [M + H$^+$].

2-[4-(4-Methylpiperazin-1-yl)-3-phenoxybenzoylamino-benzoic acid (23d) was prepared according to the general procedure for replacement of fluoro group: ^{1}H NMR (300 MHz, DMSO-d_6) δ 12.14 (s, 1H), 9.75 (br s, 1H), 8.67 (d, J = 8.4 Hz, 1H), 8.07 (d, J = 8.1 Hz, 1H), 7.77 (d, J = 8.7 Hz, 1H), 7.67 (t, J = 8.1 Hz, 1H), 7.46 (m, 3H), 7.36 (d, J = 8.4 Hz, 1H), 7.22 (t, J = 7.2 Hz, 2H), 7.07 (d, J = 8.4 Hz, 2H), 3.83 (m, 2H), 3.12 (m, 2H), 2.86 (s, 4H), 2.11 (s, 3H); LCMS (API-ES) *m/z* 432.0 [M + H$^+$].

2-[4-(3,5-Dimethylpiperazin-1-yl)-3-phenoxybenzoyl-amino]benzoic acid (23e) was prepared according to the general procedure for replacement of fluoro group: ^{1}H NMR (300 MHz, DMSO-d_6) δ 13.83 (br s, 1H), 12.16 (s, 1H), 8.99 (m, 1H), 8.69 (d, J = 8.4 Hz, 1H), 8.49 (m, 1H), 8.08 (d, J = 7.9 Hz, 1H), 7.81 (d, J = 8.4 Hz, 1H), 7.68 (t, J = 7.9 Hz, 1H), 7.56 (s, 1H), 7.44 (t, J = 7.7 Hz, 2H), 7.36 (d, J = 8.5 Hz, 1H), 7.20 (m, 2H), 7.03 (d, J = 8.4 Hz, 2H), 1.24 (d, J = 6.4 Hz, 6H); LCMS (API-ES) *m/z* 446.0 [M + H$^+$]; 444.0 [M + H$^-$].

2-(4-Morpholin-4-yl-3-phenoxybenzoylamino)benzoic acid (23f) was prepared according to the general procedure for replacement of fluoro group: ^{1}H NMR (300 MHz, DMSO-d_6) δ 12.14 (s, 1H), 8.69 (d, J = 7.8 Hz, 1H), 8.07 (dd, J = 1.5 and 7.9 Hz, 1H), 7.79 (dd, J = 2.1 and 8.5 Hz, 1H), 7.67 (m, 1H), 7.53 (d, J = 2.1 Hz, 1H), 7.42 (m, 2H), 7.14−7.27 (m, 3H), 6.99 (m, 2H), 3.17 (m, 5H); LCMS (API-ES) *m/z* 419.0 [M + H$^+$]; 417.0 [M + H$^-$].

2-(3-Phenoxy-4-thiomorpholin-4-ylbenzoylamino)benzoic acid (23g) was prepared according to the general procedure for replacement of fluoro group:^{1}H NMR (300 MHz, DMSO-d_6) δ 12.14 (s, 1H), 8.69 (d, J = 8.6 Hz, 1H), 8.07 (d, J = 7.8 Hz, 1H), 6.99−7.77 (m, 8H), 6.95 (m, 2H); LCMS (API-ES) *m/z* 433.0 [M + H$^-$].

2-(3-Phenoxy-4-piperidin-1-ylbenzoylamino)benzoic acid (23h) was prepared according to the general procedure for replacement of fluoro group: ^{1}H NMR (300 MHz, DMSO-d_6) δ 13.97 (br s, 1H), 12.14 (s, 1H), 8.70 (d, J = 8.5 Hz, 1H), 8.07 (d, J = 7.9 Hz, 1H), 7.77 (d, J = 8.5 Hz, 1H), 7.67 (t, J = 7.8 Hz, 1H), 7.53 (d, J = 1.9 Hz, 1H), 7.39 (m, 2H), 7.11−7.26 (m, 3H), 6.97 (m, 2H), 3.15 (s, 5H), 2.77 (s, 1H), 2.61 (s, 1H); LCMS (API-ES) *m/z* 417.0 [M + H$^+$]; 415.0 [M + H$^-$].

2-[4-(3,5-Dimethylpiperidin-1-yl)-3-phenoxybenzoyl-amino]benzoic acid (23i) was prepared according to the general procedure for replacement of fluoro group: ^{1}H NMR (300 MHz, DMSO-d_6) δ 12.13 (s, 1H), 8.71 (d, J = 8.2 Hz, 1H), 8.07 (dd, J = 1.5 and 7.9 Hz, 1H), 7.78 (dd, J = 2.2 and 8.4 Hz, 1H), 7.67 (t, J = 7.8 Hz, 1H), 7.56 (d, J = 2.2 Hz, 1H), 7.38 (t, J = 8.0 Hz, 2H), 7.21 (m, 2H), 7.12 (d, J = 7.3 Hz, 1H), 6.93 (m, 2H), 3.45 (overlap with DMSO water), 2.47 (m, 2H), 1.71 (m, 1H), 1.21 (m, 2H), 0.84 (d, 6H); LCMS (API-ES) *m/z* 445.0 [M + H$^+$]; 443.0 [M + H$^-$].

General Procedure for the Preparation of Derivatives 24a−p via Pd-Mediated Cross-Coupling. A mixture of 2-(4-bromo-3-phenoxybenzoylamino)benzoic acid methyl ester (**22**, 1 equiv), aryl boronic acid or ester (1.5 equiv), 2 M aqueous $NaCO_3$ (3 equiv), and $Pd(PPh_3)_4$ (3 mol %), in DME (to 0.5 M the ester, compound **22**), was heated at 85 °C under an inert atmosphere for 5 h or until HPLC or TLC analysis indicates complete reaction. The mixture was then concentrated in vacuo, dissolved in EtOAc (20 mL), washed with H_2O (2 × 5 mL) and brine (1 × 5 mL), and dried over anhydrous $MgSO_4$. The methyl ester was then hydrolyzed, and the crude material was purified using RP-HPLC.

2-[3-Phenoxy-4-(1*H*-pyrazol-4-yl)benzoylamino]benzoic acid (24a) was prepared according to the general Pd-mediated cross-coupling procedure: ^{1}H NMR (300 MHz, DMSO-d_6) δ 12.21 (s, 1H), 8.67 (d, J = 8.1 Hz, 1H), 8.18 (s, 2H), 8.07 (d, J = 8.1 Hz, 2H), 7.84 (d, J = 7.7 Hz, 1H), 7.69 (m, 1H), 7.58 (d, J = 1.7 Hz, 1H), 7.41 (t, J = 8.5 Hz, 2H), 7.17 (m, 2H), 7.07 (m, 2H); LCMS (API-ES) *m/z* 400.0 [M + H$^+$]; 398.0 [M + H$^-$].

2-(3-Phenoxy-4-pyridin-3-ylbenzoylamino)benzoic acid (24b) was prepared according to the general Pd-mediated cross-coupling procedure: ^{1}H NMR (300 MHz, DMSO-d_6) δ 12.24 (s, 1H), 8.88 (d, J = 1.6 Hz, 1H), 8.67 (d, J = 8.4 Hz, 1H), 8.62 (d, J = 8.1 Hz, 1H), 8.10 (m, 2H), 7.87 (m, 2H), 7.70 (t, J = 7.9 Hz, 1H), 7.57 (m, 2H), 7.43 (t, J = 8.0 Hz, 2H), 7.27 (t, J = 7.3 Hz, 1H), 7.20 (t, J = 7.4 Hz, 1H), 7.08 (d, J = 8.7 Hz, 2H); LCMS (API-ES) *m/z* 411.0 [M + H$^+$]; 309.0 [M + H$^-$].

2-[(2-Phenoxybiphenyl-4-carbonyl)amino]benzoic acid (24c) was prepared according to the general Pd-mediated cross-coupling procedure: ^{1}H NMR (300 MHz, DMSO-d_6) δ 12.27 (s, 1H), 8.68 (d, J = 8.4 Hz, 1H), 8.08 (dd, J = 1.5 and 7.9 Hz, 1H), 7.88 (dd, J = 1.7 and 8.1 Hz, 1H), 7.77 (d, J = 8.0 Hz, 1H), 7.38−7.69 (m, 9H), 7.26 (t, J = 7.8 Hz, 1H), 7.17 (t, J = 7.9 Hz, 1H), 7.05 (m, 2H); LCMS (API-ES) *m/z* 410.0 [M + H$^+$]; 408.0 [M + H$^-$].

2-[(2-Phenoxy-4′-trifluoromethylbiphenyl-4-carbonyl)-amino]benzoic acid (24d) was prepared according to the general Pd-mediated cross-coupling procedure: ^{1}H NMR (300 MHz, DMSO-d_6) δ 13.98 (br s, 1H), 12.30 (s, 1H), 8.67 (d, J = 8.3 Hz, 1H), 8.08 (dd, J = 1.4 and 7.9 Hz, 1H), 7.82−7.91 (m, 6H), 7.67 (t, J = 7.7 Hz, 1H), 7.57 (d, J = 1.3 Hz, 1H), 7.43 (t, J = 7.9 Hz, 2H), 7.19 (t, J = 7.4 Hz, 1H), 7.11 (t, J = 7.0 Hz, 1H), 6.98 (d, J = 8.5 Hz, 2H); LCMS (API-ES) *m/z* 478.0 [M + H$^+$]; 476.0 [M + H$^-$].

2-[(4′-Methyl-2-phenoxybiphenyl-4-carbonyl)amino]-benzoic acid (24e) was prepared according to the general Pd-mediated cross-coupling procedure: ^{1}H NMR (300 MHz, DMSO-d_6) δ 13.85 (br s, 1H), 12.25 (s, 1H), 8.68 (d, J = 8.4 Hz, 1H), 8.08 (d, J = 7.9 Hz, 1H), 7.87 (d, J = 8.1 Hz, 1H), 7.72 (m, 2H), 7.55 (d, J = 8.3 Hz, 3H), 7.40 (t, J = 7.8 Hz, 2H), 7.26 (m, 3H), 7.15 (t, J = 7.3 Hz, 1H), 7.03 (d, J = 8.5 Hz, 2H), 2.36 (s, 3H); LCMS (API-ES) *m/z* 424.0 [M + H$^+$]; 422.0 [M + H$^-$].

4′-(2-Carboxyphenylcarbamoyl)-2′-phenoxybiphenyl-4-carboxylic acid (24f) was prepared according to the general Pd-mediated cross-coupling procedure: ^{1}H NMR (300 MHz, DMSO-d_6) δ 13.89 (br s, 1H), 13.08 (br s, 1H), 12.27 (s, 1H), 8.67 (d, J = 7.8 Hz, 1H), 8.08 (dd, J = 1.5 and 7.9 Hz, 1H), 8.03 (d, J = 8.4 Hz, 2H), 7.89 (dd, J = 1.6 and 8.1 Hz, 1H), 7.80 (t, J = 9.1 Hz, 3H), 7.70 (dt, J = 1.6 and 7.9 Hz, 1H), 7.55 (ds, J = 1.5 Hz, 1H), 7.42 (t, J = 8.0 Hz, 2H), 7.23 (dt, J = 1.0 and 7.8 Hz, 1H), 7.17 (t, J = 7.4 Hz, 1H), 7.07 (dd, J = 1.0 and 8.6 Hz, 2H); LCMS (API-ES) *m/z* 454.0 [M + H$^+$]; 452.0 [M + H$^-$].

2-[(4′-Hydroxy-2-phenoxybiphenyl-4-carbonyl)amino]-benzoic acid (24g) was prepared according to the general Pd-mediated cross-coupling procedure: ^{1}H NMR (300 MHz, DMSO-d_6) δ 12.23 (s, 1H), 9.69 (s, 1H), 8.69 (d, J = 8.4 Hz, 1H), 8.07 (d, J = 7.9 Hz, 1H), 7.84 (d, J = 8.0 Hz, 1H), 7.69 (m, 2H), 7.56 (s, 1H), 7.49 (d, J = 7.9 Hz, 2H), 7.40 (t, J = 7.5 Hz, 2H), 7.25 (t, J = 7.7 Hz, 1H), 7.14 (t, J = 7.1 Hz, 1H), 7.01 (d, J = 8.0 Hz, 2H), 6.84 (d, J = 8.0 Hz, 2H); LCMS (API-ES) *m/z* 425.9 [M + H$^+$]; 424.0 [M + H$^-$].

2-[(4′-Ethoxy-2-phenoxybiphenyl-4-carbonyl)amino]-benzoic acid (24h) was prepared according to the general Pd-mediated cross-coupling procedure: ^{1}H NMR (300 MHz, DMSO-d_6) δ 12.29 (s, 1H), 8.68 (d, J = 8.1 Hz, 1H), 8.07 (dd, J = 1.4 and 7.9 Hz, 1H), 7.85 (dd, J = 1.6 and 8.1 Hz, 1H), 7.73 (d, J = 8.0 Hz, 1H), 7.68 (t, J = 7.9 Hz, 1H), 7.56 (m, 3H), 7.40 (t, J = 7.9 Hz, 2H), 7.17 (t, J = 7.8 Hz, 1H), 7.15 (t, J = 7.6 Hz, 1H), 7.00 (m, 4H), 4.07 (q, J = 6.9 Hz, 2H), 1.37 (t, J = 6.9 Hz, 3H); LCMS (API-ES) *m/z* 454.0 [M + H$^+$]; 452.0 [M + H$^-$].

2-[(4′-Methanesulfonyl-2-phenoxybiphenyl-4-carbonyl)amino]benzoic acid (24i) was prepared according to the general Pd-mediated cross-coupling procedure: ^{1}H NMR (300 MHz, DMSO-d_6) δ 13.85 (br s, 1H), 12.25 (s, 1H), 8.66 (d, J = 8.0 Hz, 1H), 8.08 (dd, J = 1.5 and 7.9 Hz, 1H), 8.04 (d, J = 8.4 Hz, 2H), 7.94 (d, J = 8.4 Hz, 2H), 7.89 (dd, J = 1.5 and 8.1 Hz, 1H), 7.83 (d, J = 8.0 Hz, 1H), 7.70 (dt, J = 1.5 and 7.9 Hz, 1H), 7.55 (ds, J = 1.4 Hz, 1H), 7.45 (t, J = 7.7 Hz, 2H), 7.23 (p, J = 7.5 Hz, 2H), 7.12 (d, J = 7.8 Hz, 2H), 3.30 (s, 3H); LCMS (API-ES) *m/z* 488.0 [M + H$^+$]; 485.9 [M + H$^-$].

2-[(3′-Isopropyl-2-phenoxybiphenyl-4-carbonyl)amino]-benzoic acid (24j) was prepared according to the general Pd-mediated cross-coupling procedure: ^{1}H NMR (300 MHz, DMSO-d_6) δ 13.85 (br s, 1H), 12.26 (s, 1H), 8.68 (d, J = 8.1 Hz, 1H), 8.08 (d, J = 7.8 Hz, 1H), 7.88 (d, J = 8.2 Hz, 1H), 7.79 (m, 2H), 7.61 (s, 1H), 7.41 (m, 5H), 7.28 (m, 2H), 7.18 (t, J = 7.6 Hz, 1H), 7.03 (d, J = 8.1 Hz, 2H), 2.80 (m, 1H), 1.21 (d, J = 3.4 Hz, 6H); LCMS (API-ES) *m/z* 452.0 [M + H$^+$]; 450.0 [M + H$^-$].

2-[(2-Phenoxy-3′-trifluoromethoxybiphenyl-4-carbonyl)-amino]benzoic acid (24k) was prepared according to the general Pd-mediated cross-coupling procedure: ^{1}H NMR (300 MHz, DMSO-d_6) δ 13.85 (br s, 1H), 12.26 (s, 1H), 8.67 (d, J = 8.1 Hz, 1H), 8.08 (dd, J = 1.5 and 7.9 Hz, 1H), 7.89 (dd, J = 1.5 and 8.1 Hz, 1H), 7.83 (d, J = 8.0 Hz, 1H), 7.70 (m, 2H), 7.64 (m, 2H), 7.58 (m, 1H), 7.42 (t, J = 7.8 Hz, 3H), 7.26 (t, J = 7.3 Hz, 1H), 7.18 (t, J = 7.4 Hz, 1H), 7.07 (d, J = 7.9 Hz, 2H); LCMS (API-ES) *m/z* 493.9 [M + H$^+$]; 491.9 [M + H$^-$].

2-[(4′-Fluoro-3′-methyl-2-phenoxybiphenyl-4-carbonyl)-amino]benzoic acid (24l) was prepared according to the general Pd-mediated cross-coupling procedure: ^{1}H NMR (300 MHz, DMSO-d_6) δ 13.98 (br s, 1H), 12.24 (s, 1H), 8.68 (d, J = 8.2 Hz, 1H), 8.08 (dd, J = 1.6 and 7.9 Hz, 1H), 7.86 (dd, J = 1.7 and 8.1 Hz, 1H), 7.76 (d, J = 6.1 Hz, 1H), 7.69 (dt, J = 1.6 and 7.9 Hz, 1H), 7.57 (dd, J = 2.0 and 8.3 Hz, 2H), 7.50 (m, 1H), 7.41 (t, J = 7.6 Hz, 2H), 7.14−7.27 (m, 3H), 7.04 (d, J = 7.7 Hz, 2H), 2.29 (s, 3H); LCMS (API-ES) *m/z* 442.0 [M + H$^+$]; 440.0 [M + H$^-$].

2-[(3′-Chloro-4′-fluoro-2-phenoxybiphenyl-4-carbonyl)-amino]benzoic acid (24m) was prepared according to the general Pd-mediated cross-coupling procedure: ^{1}H NMR (300 MHz, DMSO-d_6) δ 13.79 (br s, 1H), 12.29 (s, 1H), 8.67 (d, J = 8.5 Hz, 1H), 8.08 (d, J = 7.9 Hz, 1H), 7.83 (m, 3H), 7.69 (m, 2H), 7.55 (m, 2H), 7.44 (t, J = 7.0 Hz, 2H), 7.22 (m, 2H), 7.08 (d, J = 8.0 Hz, 2H); LCMS (API-ES) *m/z* 461.9, 463.9 [M + H$^+$]; 460.0, 461.9 [M + H$^-$].

2-[(3′,4′-Difluoro-2-phenoxybiphenyl-4-carbonyl)amino]benzoic acid (24n) was prepared according to the general Pd-mediated cross-coupling procedure: ^{1}H NMR (300 MHz, DMSO-d_6) δ 13.98 (br s, 1H), 12.26 (s, 1H), 8.66 (d, J = 8.3 Hz, 1H), 8.08 (dd, J = 1.5 and 7.9 Hz, 1H), 7.69−7.85 (m, 4H), 7.52−7.58 (m, 3H), 7.43 (t, J = 7.9 Hz, 2H), 7.25 (t, J = 8.2 Hz, 1H), 7.25 (t, J = 7.6 Hz, 1H), 7.07 (d, J = 8.6 Hz, 2H); LCMS (API-ES) *m/z* 446.0 [M + H$^+$]; 443.9 [M + H$^-$].

2-[(4′-Chloro-3′-methyl-2-phenoxybiphenyl-4-carbonyl)-amino]benzoic acid (24o) was prepared according to the general Pd-mediated cross-coupling procedure: ^{1}H NMR (300 MHz, DMSO-d_6) δ 13.86 (br s, 1H), 12.25 (s, 1H), 8.67 (d, J = 8.1 Hz, 1H), 8.08 (dd, J = 1.5 and 7.9 Hz, 1H), 7.86 (dd, J = 1.7 and 8.1 Hz, 1H), 7.77 (d, J = 8.0 Hz, 1H), 7.69 (t, J = 8.1 Hz, 1H), 7.64 (s, 1H), 7.56 (d, J = 1.6 Hz, 1H), 7.50 (d, J = 1.1 Hz, 2H), 7.40 (m, 2H), 7.26 (t, J = 7.9 Hz, 1H), 7.18 (t, J = 7.4 Hz, 1H), 7.04 (d, J = 7.7 Hz, 2H), 2.39 (s, 3H); LCMS (API-ES) *m/z* 458.0, 460.0 [M + H$^+$]; 455.9, 458.0 [M + H$^-$].

2-[(2′,4′-Difluoro-2-phenoxybiphenyl-4-carbonyl)amino]benzoic acid (24p) was prepared according to the general Pd-mediated cross-coupling procedure: ^{1}H NMR (300 MHz, DMSO-d_6) δ 13.85 (br s, 1H), 12.25 (s, 1H), 8.66 (d, J = 7.6 Hz, 1H), 8.08 (dd, J = 1.5 and 7.9 Hz, 1H), 7.85 (dd, J = 1.7 and 8.0 Hz, 1H), 7.71 (d, J = 8.1 Hz, 2H), 7.61 (m, 1H), 7.53 (ds, J = 1.6 Hz, 1H), 7.43 (m, 3H), 7.23 (m, 3H), 7.04 (d, J = 7.7 Hz, 2H); LCMS (API-ES) *m/z* 446.0 [M + H$^+$]; 444.0 [M + H$^-$].

Pyridin-4-yloxybenzoic Acid (25). To a solution of methyl 3-hydroxybenzoate (**16**, 609 mg, 4 mmol) in dry pyridine was added NaH (60%, 200 mg, 5 mmol). The reaction mixture was stirred at room temperature for 0.5 h. Then chloropyridine hydrochloride (600 mg, 4 mmol) was added, followed with a catalytic amount of CuCl (100 mg). The reaction mixture was allowed to heat at 120 °C for 24 h. The reaction mixture was cooled and separated between EtOAc and H_2O. Combined organic layers were washed with brine and H_2O, dried over anhydrous $MgSO_4$, and concentrated in vacuo. The crude material was then saponified and purified using RP-HPLC: ^{1}H NMR (300 MHz, DMSO-d_6) δ 8.58 (dd, J = 4.8 Hz, 2H), 7.93 (dd, J = 1.3 and 7.6 Hz, 1H), 7.70 (m, 2H), 7.56 (m, 1H), 7.08 (m, 2H); LCMS (API-ES) *m/z* 216.1 [M + H$^+$]; 214.1 [M + H$^-$].

2-(3-Bromobenzoylamino)benzoic Acid Methyl Ester (27). Using the general procedure for amide formation, starting material 3-bromobenzoic acid (**26**, 2 g, 10 mmol) was first converted to acetyl chloride, followed by reaction with methyl anthranilate (1.16 mL, 9 mmol) to give 2.6 g of product (**27**, 78%): ^{1}H NMR (300 MHz, DMSO-d_6) δ 11.50 (s, 1H), 8.45 (d, J = 8.3 Hz, 1H), 8.14 (t, J = 3.5 Hz, 1H), 8.03 (dd, J = 1.5 and 7.9 Hz, 1H), 7.98 (md, J = 7.3 Hz, 1H), 7.92 (md, J = 7.5 Hz, 1H), 7.72 (dt, J = 8.1 Hz, 1H), 7.62 (t, J = 7.9 Hz, 1H), 7.34 (dt, J = 7.9 Hz, 1H), 3.92 (s, 3H); LCMS (API-ES) *m/z* 333.9, 335.9 [M + H$^+$]; 331.9, 333.9 [M + H$^-$].

3-(3-Phenoxybenzoylamino)thiophene-2-carboxylic acid (28a) was prepared according to the general procedure for amide bond formation: ^{1}H NMR (300 MHz, DMSO-d_6) δ 13.70 (br s, 1H), 11.23 (s, 1H), 8.09 (d, J = 5.4 Hz, 1H), 7.96 (d, J = 5.0 Hz, 1H), 7.68 (m, 2H), 7.52 (m, 1H), 7.48 (d, J = 7.6 Hz, 2H), 7.34 (m, 1H), 7.26 (dt, J = 1.0 and 7.4 Hz, 1H), 7.15 (d, J = 7.7 Hz, 2H); LCMS (API-ES) *m/z* 340.0 [M + H$^+$]; 338.0 [M + H$^-$].

2-(3-Phenoxybenzoylamino)thiophene-3-carboxylic acid (28b) was prepared according to the general procedure for amide bond formation: ^{1}H NMR (300 MHz, DMSO-d_6) δ 13.45 (br s, 1H), 12.08 (s, 1H), 7.69 (m, 2H), 7.50 (dt, J = 1.2 and 7.1 Hz, 3H), 7.37 (m, 1H), 7.27 (m, 2H), 7.14 (q, J = 8.4 Hz, 3H); LCMS (API-ES) *m/z* 340.0 [M + H$^+$]; 338.0 [M + H$^-$].

3-(3-Phenoxybenzoylamino)pyridine-2-carboxylic acid (28c) was prepared according to the general procedure for amide bond formation: ^{1}H NMR (300 MHz, DMSO-d_6) δ 12.62 (s, 1H), 9.12 (d, J = 8.3 Hz, 1H), 8.47 (d, J = 3.9 Hz, 1H), 7.83 (q, J = 4.7 Hz, 1H), 7.77 (d, J = 7.8 Hz, 1H), 7.67 (t, J = 8.0 Hz, 1H), 7.58 (s, 1H), 7.49 (t, J = 7.9 Hz, 2H), 7.35 (dd, J = 2.1, 7.8 Hz, 1H), 7.25 (t, J = 7.4 Hz, 1H), 7.14 (d, J = 7.9 Hz, 2H); LCMS (API-ES) *m/z* 335.0 [M + H$^+$]; 333.0 [M + H$^-$].

2-(3-Phenoxybenzoylamino)nicotinic acid (28d) was prepared according to the general procedure for amide bond formation: ^{1}H NMR (300 MHz, DMSO-d_6) δ 11.54 (s, 1H), 8.61 (d, J = 8.3 Hz, 1H), 8.26 (dd, J = 1.8 and 7.7 Hz, 1H), 7.80 (d, J = 7.8 Hz, 1H), 7.59 (m, 2H), 7.47 (m, 2H), 7.24 (m, 2H), 7.14 (t, J = 7.6 Hz, 1H), 7.05 (m, 2H); LCMS (API-ES) *m/z* 335.0 [M + H$^+$]; 333.0 [M + H$^-$].

2-Fluoro-6-(3-phenoxybenzoylamino)benzoic acid (28e) was prepared according to the general procedure for amide bond formation: ^{1}H NMR (300 MHz, DMSO-d_6) δ 13.75 (br s, 1H), 11.16 (s, 1H), 7.92 (d, J = 8.2 Hz, 1H), 7.74 (d, J = 7.8 Hz, 1H), 7.62 (m, 2H), 7.57 (m, 1H), 7.49 (t, J = 8.1 Hz, 2H), 7.30 (dd, J = 2.5 and 8.1 Hz, 1H), 7.24 (t, J = 7.6 Hz, 1H), 7.13 (m, 3H); LCMS (API-ES) *m/z* 352.0 [M + H$^+$]; 350.0 [M + H$^-$].

2-Hydroxy-6-(3-phenoxybenzoylamino)benzoic Acid (28f). To a suspension of 3-phenoxybenzoyl chloride (550 mg, 2.37 mmol) in dry pyridine (3 mL) was added 2-amino-6-methoxybenzoic acid methyl ester (264 mg, 1.58 mmol) at 0 °C. After stirring for 24 h at room temperature, the reaction mixture was concentrated, taken up in EtOAc, and washed with H_2O and 1 N HCl. The organics were washed with brine, dried over anhydrous $MgSO_4$, and concentrated in vacuo. The residue was then dissolved in THF (4 mL) and treated with 1 N LiOH (3.46 mL, 3.46 mmol). After stirring overnight at room temperature, the reaction mixture was concentrated and separated between EtOAc and H_2O. The organic layers were dried and concentrated to give 382 mg of the intermediate, 2-methoxy-6-(3-phenoxybenzoylamino)benzoic acid (67%). To this intermediate (161 mg, 0.44 mmol) in DCM (5 mL) at 0 °C was added boron tribromide (1 M in DCM, 0.66 mL, 0.66 mmol) dropwise. After stirring at room temperature for 2 h, MeOH was added to quench the reaction. The reaction mixture was trituated (3×) with MeOH and the crude material was purified using RP-HPLC to give 20 mg of product (13%): ^{1}H NMR (300 MHz, DMSO-d_6) δ 13.23 (s, 1H), 7.98 (d, J = 8.2 Hz, 1H), 7.76 (d, J = 8.2 Hz, 1H), 7.57−7.63 (m, 2H), 7.45−7.51 (m, 2H), 7.21−7.33 (m, 3H), 7.13 (m, 2H), 6.59 (d, J = 8.1 Hz, 1H); LCMS (API-ES) *m/z* 349.6 [M + H$^+$]; 347.6 [M + H$^-$].

2-[3-(Pyridin-4-yloxy)benzoylamino]benzoic acid (28g) was prepared according to the general procedure for amide bond formation using **25** as starting material: ^{1}H NMR (300 MHz, DMSO-d_6) δ 12.24 (s, 1H), 8.75 (d, J = 6.4 Hz, 2H), 8.69 (d, J = 8.0 Hz, 1H), 8.09 (dd, J = 1.5 and 7.9 Hz, 1H), 7.98 (d, J = 8.0 Hz, 1H), 7.84 (m, 2H), 7.72 (dt, 1H), 7.64 (dd, 1H), 7.40 (m, 2H), 7.28 (dt, 1H); LCMS (API-ES) *m/z* 335.0 [M + H$^+$]; 333.0 [M + H$^-$].

2-[3-(3-Carboxyphenoxy)benzoylamino]benzoic Acid (28h). Representative Procedure for 28h−j. To a stirred solution of methyl 3-hydroxybenzoate (152 mg, 1.00 mmol) in pyridine (5 mL) was added NaH (60 mg, 1.5 mmol), and the reaction mixture was stirred for 30 min. At the conclusion of this time, 2-(3-bromobenzoylamino)benzoic acid methyl ester (**27**, 334 mg, 1.00 mmol) and CuCl (99 mg, 1.00 mmol) were added, and the reaction mixture was stirred at 120 °C for 2 days. The reaction mixture was removed from the heat, neutralized with 1 N HCl, and extracted with EtOAc (3×). The organics were washed with brine, dried over anhydrous $MgSO_4$, and concentrated in vacuo. LCMS confirmed the formation of the hydrolyzed material (in the case of **28i** and **28j**, final compounds were obtained after sponification). This material was then purified using RP-HPLC to afford the final compound **28h** (54 mg, 14%): ^{1}H NMR (300 MHz, DMSO-d_6) δ 13.85 (br s, 1H), 13.25 (br s, 1H), 12.21 (s, 1H), 8.69 (dd, J = 0.7 and 7.7 Hz, 1H), 8.09 (dd, J = 1.5 and 7.9 Hz, 1H), 7.80 (m, 2H), 7.70 (m, 2H), 7.63 (m, 1H), 7.60 (d, J = 7.9 Hz, 1H), 7.54 (m, 1H), 7.40 (m, 2H), 7.26 (t, J = 7.3 Hz, 1H); LCMS (API-ES) *m/z* 377.9 [M + H$^+$]; 376.0 [M + H$^-$].

2-[3-(4-Carboxyphenoxy)benzoylamino]benzoic acid (28i): ^{1}H NMR (300 MHz, DMSO-d_6) δ 12.21 (s, 1H), 8.69 (d, J = 8.3 Hz, 1H), 8.00 (m, 3H), 7.73 (d, J = 7.5 Hz, 1H), 7.66 (m, 3H), 7.45 (dd, J = 2.2 and 8.0 Hz, 1H), 7.26 (t, J = 7.6 Hz, 1H), 7.16 (m, 2H); LCMS (API-ES) *m/z* 377.9 [M + H$^+$]; 376.0 [M + H$^-$].

2-[3-(4-Fluorophenoxy)benzoylamino]benzoic acid (28j): ^{1}H NMR (300 MHz, DMSO-d_6) δ 12.22 (s, 1H), 8.69 (dd, J = 0.8 and 8.4 Hz, 1H), 8.08 (dd, J = 1.5 and 7.9 Hz, 1H), 7.61−7.75 (m, 3H), 7.54 (t, J = 2.0 Hz, 1H), 7.18−7.35 (m, 6H); LCMS (API-ES) *m/z* 352.0 [M + H$^+$]; 350.0 [M + H$^-$].

2-(4-Bromo-3-phenoxybenzoylamino)-6-methoxybenzoic acid (30). The acid (**20**, 668 mg, 2.28 mmol) was converted to the acid chloride by refluxing in thionyl chloride with 3 drops of DMF. After 2 h, the reaction mixture was concentrated and suspended in pyridine. The mixture was cooled to 0 °C under N_2, and 2-amino-6-methoxybenzoic acid (334 mg, 2 mmol) was added. After stirring for 24 h at room temperature, the reaction mixture was concentrated, neutralized with 1 N HCl, and extracted with EtOAc (3×). The organics were washed with brine, dried over anhydrous $MgSO_4$, and concentrated in vacuo. The cyclized intermediate (**29**) was then hydrolyzed with 1 N LiOH (7 mL, 6.84 mmol) in THF overnight. The reaction mixture was concentrated, acidified by 1 N HCl (10 mL), and extracted by EtOAc. The final compound was purified using RP-HPLC to provide 150 mg of product (**30**, 15% in three steps): ^{1}H NMR (300 MHz, DMSO-d_6) δ 13.05 (br s, 1H), 10.76 (s, 1H), 8.00 (d, J = 8.2 Hz, 1H), 7.70 (dd, J = 2.0 and 8.3 Hz, 1H), 7.56 (d, J = 2.0 Hz, 1H), 7.40−7.49 (m, 3H), 7.18−7.28 (m, 2H), 6.92−7.07 (m, 3H), 3.90 (s, 3H); LCMS (API-ES) *m/z* 441.4, 443.5 [M + H$^+$]; 439.5, 441.5 [M + H$^-$].

2-(4-Bromo-3-phenoxybenzoylamino)-6-hydroxybenzoic Acid (31). To compound **30** (50 mg, 0.11 mmol) in DCM (3 mL) at 0 °C was added boron tribromide (1 M in DCM, 0.17 mL, 0.17 mmol) dropwise. After stirring at room temperature for 20 h, MeOH was added to quench the reaction. Reaction mixture was trituated three times with MeOH and the crude material was purified using RP-HPLC to give 20 mg of product (42%): ^{1}H NMR (300 MHz, DMSO-d_6) δ 13.37 (s, 1H), 7.99 (d, J = 8.3 Hz, 1H), 7.88 (d, J = 8.2 Hz, 1H), 7.74 (d, J = 8.3 Hz, 1H), 7.56 (d, J = 1.7 Hz, 1H), 7.47 (t, J = 7.9 Hz, 2H), 7.24−7.32 (m, 2H), 7.07 (d, J = 8.4 Hz, 2H), 6.60 (d, J = 8.2 Hz, 1H); LCMS (API-ES) *m/z* 427.4, 429.5 [M + H$^+$]; 425.5, 427.4 [M + H$^-$].

2-Hydroxy-6-[(2-phenoxybiphenyl-4-carbonyl)amino]-benzoic Acid (33). Using the general Pd-mediated cross-coupling procedure, 100 mg of compound **30** (0.22 mmol) was coupled with phenylboronic acid (50 mg, 0.4 mmol) to give the intermediate (**32**, 37 mg). This was then treated with boron tribromide (1 M in DCM, 0.16 mL, 0.16 mmol) in DCM. Purification by RP-HPLC provided 10 mg of final product (**33**, 11%): ^{1}H NMR (300 MHz, DMSO-d_6) δ 13.79 (s, 1H), 7.97 (d, J = 7.8 Hz, 1H), 7.89 (dd, J = 1.4 and 8.1 Hz, 1H), 7.72 (d, J = 8.0 Hz, 1H), 7.66 (m, 2H), 7.57 (d, J = 1.5 Hz, 1H), 7.40−7.49(m, 5H), 7.26 (t, J = 8.2 Hz, 1H), 7.14 (t, J = 8.2 Hz, 1H), 7.04 (d, J = 8.0 Hz, 2H), 6.56 (dd, J = 0.8 and 8.2 Hz, 1H); LCMS (API-ES) *m/z* 425.5 [M + H$^+$]; 423.6 [M + H$^-$].

Computational Chemistry Methods. Protein and small molecule modeling visualization was accomplished with Sybyl v. 6.7 (Tripos, Inc. St. Louis, MO.) and Macromodel v. 4.1 (Schrödinger, Inc. Portland, OR.). Handling of the small molecule virtual library, calculations of Lipinski properties, conversion of the library from 2D to 3D structures, similarity/substructure search, and pharmacophore modeling were accomplished by the Unity 4.2, CONCORD, and HiVol modules in the Tripos suite (Tripos, Inc. St. Louis, MO.). Docking was done using FlexX in Sybyl v. 6.7. Conformational analysis and clustering were performed in Macromodel v. 4.1 (Schrödinger, Inc. Portland, OR.).

Expression and Purification of ACP, ACPS, FabD, and FabH. Full-length *E. coli* acyl carrier protein (ACP), acyl carrier protein synthase (ACPS), malonyl-CoA:ACP transacylase (FabD), and 3-ketoacyl-ACP synthase III (FabH) were individually cloned into pET expression vectors (Novagen) with an N-terminal His-tag (ACP, ACPS in pET19; FabD, FabH in pET28). *E. coli* FabH was also cloned in a tagless version in pET30 vector. *E. faecalis*, *S. pyogenes*, *S. aureus.*, *H. influenzae* FabHs were also cloned and expressed in pET vector in both His-tagged (pET28) and tagless (pET30) versions.

All proteins were expressed in *E. coli* strain BL21(DE3) (Invitrogen). Harvested cells containing His-tagged ACP, ACPS, FabD, and FabHs were lysed by sonication in 20 mM Tris, pH 7.6, 5 mM imidazole, 0.5 M NaCl and centrifuged at 20 000 rpm for 30 min. The supernatant was applied to a Ni−NTA agarose column (Qiagen), washed, and eluted using a 5−500 mM imidazole gradient over 20 column volumes. Eluted protein was dialyzed against 20 mM Tris, pH 7.6, 1 mM DTT, and 100 mM NaCl. Purified FabD and FabHs were concentrated up to 2 mg/mL and stored at −80°C in 20 mM Tris, pH 7.6, 100 mM NaCl, 1 mM DTT, and 20% glycerol for enzymatic assays.

Harvested cells expressing tagless FabHs were sonicated in 25 mM Tris, pH 8.0, 20 mM NaCl, 2 mM DTT, 1 mM EDTA, 50 mM β-ME, and 0.5 mL (per 100 mL lysate) protease inhibitor cocktail (Roche). The crude lysate was centrifuged at 20 000 rpm for 30 min, and the soluble fraction was separated by anion exchange chromatography (HiPrep 16/10 Q XL, Amersham Pharmacia Biotech, (APB)) using a 0−1 M NaCl gradient over 10 column volumes. Protein fractions were checked by SDS−PAGE, and appropriate fractions were dialyzed against 25 mM Tris, pH 8.0, 2 mM DTT, and 50 mM β-ME. Dialyzed protein was loaded onto a 10-mL Source Q-15 column (APB) and further separated by anion-exchange chromatography using a 0−500 mM NaCl gradient over 20 column volumes. Protein fractions were checked by SDS−PAGE, and FabH-containing fractions were pooled and loaded onto an 8-mL hydroxyapaptite column (Bio-Rad) and eluted with a 0−250 mM gradient of a pH 8.0 potassium phosphate buffer over 15 column volumes. FabH-containing fractions were concentrated up to 2 mg/mL and stored at −80 °C in 20 mM Tris, pH 7.6, 100 mM NaCl, 1 mM DTT, and 20% glycerol for enzymatic assays or concentrated up to 20 mg/mL for crystallization trials.

Conversion of Apo-ACP to Holo-ACP. Purified ACP contains approximately 50% of the apo-form that needs to be converted into the holo-form. The conversion reaction is catalyzed by ACP synthase (ACPS) and transfers a pantothenoate prosthetic group to apo-ACP to form holo-ACP. This method was described previously[20] and modified as follows: In the final volume of 50 mL, 50 mg ACP, 50 mM Tris, pH 9.0, 2 mM DTT, 10 mM $MgCl_2$, 600 μM CoA, and 0.2 μM ACPS was incubated for 1 h at 37 °C. The pH of the reaction was then adjusted to approximately 7.0 using 1 M potassium phosphate, pH 6. Holo-ACP was purified by fractionation of the reaction mixture by Source Q-15 (Amersham Pharmacia) ion exchange chromatography using a 0−500 mM NaCl gradient over 25 column volumes. This step not only removes ACPS, it also eliminates minor contamination of FabD and FabH-like activity that causes the elevation of background in subsequent FabD or FabH assays. Separated apo- and holo-ACPs can be detected by native polyacrylamide gel electrophoresis as described.[21]

FabD/FabH Coupled Assay. All FabH proteins purified, tagged or tagless, can use *E.coli* holo-ACP as their substrate. There is no detectable difference between tagged and tagless FabHs in terms of their enzyme activity. We coupled the FabD and FabH reactions because malonyl-ACP, the product of FabD reaction, is unstable. In a final 100-μL reaction, 100 mM Na_2HPO_4/NaH_2PO_4, pH 7.0, 2 mM DTT, 1 mM $MgCl_2$, and 12.5 μM holo-ACP were mixed with 10 nM FabD and 1−20 nM FabH (0.5−1 nM for *E. coli* FabH, 3−5 nM for *E. faecalis* and *H. influenzae* FabHs, 10 nM for *S. pyog*enes FabH, and 20 nM for *Staph. aureus* FabH), and H_2O was added to 80 μL. FabD reaction was initialized by adding 10 μL of 1 mM malonyl-CoA. After 1 min incubation, a 10 μL mixture of 125 μM acetyl-CoA, 0.75 μCi [^{3}H]acetyl-CoA (Amersham), 2.5 mM NADH, and 2.5 mM NADPH was added for FabH reaction for 19 min. The reaction was stopped by adding 100 μL of ice-cold 50% TCA, incubating for 5 min on ice, and centrifuging to pellet the protein. The pellet was washed with 10% ice-cold TCA and resuspended with 20 μL of 2 M NaOH. The incorporation of the ^{3}H signal in the final product was read by liquid scintillation. When determining the inhibition constant (IC_{50}), inhibitors were added from a concentrated DMSO stock such that the final concentration of DMSO did not exceed 2%.

Acetylation of FabH by Acetyl-CoA. To ensure that FabD was not inhibited during this coupled assay, inhibition of FabH acetylation was demonstrated. The first step of the FabH catalytic reaction is the acetylation of the catalytic cysteine residue at the active site. In the absence of holo-ACP, the reaction can be arrested at this intermediate stage. The acetylation reaction can be detected by mixing 1 μM FabH (freshly desalted to remove DTT by a PD10 desalting column (Pierce)), 100 mM, pH 7.0 sodium phosphate buffer, 1 mM $MgCl_2$ in 10−100 μL volume and initiated by adding 1−5 μM [^{3}H]acetyl-CoA (Amersham). The reaction proceeded from 1 to 10 min before being stopped by ice-cold 50% TCA, and the incorporation of radiolabel was determined by liquid scintillation as described in the previous section. A dose-dependent decrease in incorporated radiolabel indicated specific FabH inhibition.

Crystallization of FabH. All crystals were obtained by vapor diffusion using 20 mg/mL protein solution in the hanging drop setups at 15° C. The cocrystal structure of *E. faecalis* FabH with bound compound **13a** was obtained using the N-terminally His-tagged protein. The crystallization conditions consisted of 0.2 M lithium sulfate, 0.1 M Bis-Tris, pH 6.5, 25% PEG3350. The structure of *E. faecalis* FabH with bound compound **23i** was determined using the tagless protein with two specific mutations (D36A, E37A) crystallized with 25% PEG 3350, 0.2 M ammonium sulfate and 0.1 M Bis-Tris, pH 5.5.

Crystallization, Data Collection and Structure Determination. All data were collected at 110 K using MAR image plate and rotating anode X-ray generator. Crystals were frozen in synthetic mother liquor with 25% glycerol. Data were integrated, reduced, and scaled using the HKL program suite.[22] CNX was used for molecular replacement and refinement of structures. The structure of the *E. coli* FabH was first determined by molecular replacement using the 1.8 Å published structure of the same protein[10] as the starting model. All the subsequent structures were determined by molecular replacement, using the *E. coli* FabH structure as the starting model.

Acknowledgment. The authors thank Dr. Paul Brett for invaluable contributions to the project and Dr. James Levin and Cindy Atwell of our Preclinical Microbiology Department for MIC determinations and fruitful discussions. The authors also want to thank Miss Lucy Aguirre for her assistance in crystallization of FabH.

References

(1) Cronan, J. E., Jr.; Rock, C. O. In *Escherichia coli* and *Salmonella typhimurium*: Cellular and molecular biology; Neidhardt, F. C., Ingraham, I. L., Low, K. B., et al., Eds.; American Society of Microbiology: Washington, DC, 1996; pp 612−636.

(2) Joshi, A. K.; Witkowski, A.; Smith, S. Mapping of Functional Interactions Between Domains of the Animal Fatty Acid Synthase by Mutant Complementation in Vitro. *Biochemistry* **1997**, *36* (8), 2316−2322.

(3) Jackowski, S.; Murphy, C. M.; Cronan, J. E., Jr.; Rock, C. O. Acetoacetyl-acyl Carrier Protein Synthase. A Target for the Antibiotic Thiolactomycin.*J Biol. Chem*. **1989**, *264* (13), 7624−7629.

(4) Heath, R. J.; White, S. W.; Rock, C. O. Inhibitors of Fatty Acid Synthesis as Antimicrobial Chemotherapeutics. *Appl. Microbiol. Biotechnol*. **2002**, *58* (6), 695−703.

(5) Tsay, J. T.; Oh, W.; Larson, T. J.; Jackowski, S.; Rock, C. O. Isolation and Characterization of the Beta-ketoacyl-acyl Carrier Protein Synthase III Gene (fabH) from Escherichia Coli K-12. *J. Biol. Chem*. **1992**, *267* (10), 6807−6814.

(6) Price, A. C.; Choi, K. H.; Heath, R. J.; Li, Z.; White, S. W.; Rock, C. O. Inhibition of Beta-ketoacyl-acyl Carrier Protein Synthases by Thiolactomycin and Cerulenin. Structure and Mechanism. *J. Biol. Chem*. **2001**, *276* (9), 6551−6559.

(7) Khandekar, S. S.; Gentry, D. R.; Van Aller, G. S.; Warren, P.; Xiang, H.; Silverman, C.; Doyle, M. L.; Chambers, P. A.; Konstantinidis, A. K.; Brandt, M.; Daines, R. A.; Lonsdale, J. T.; Identification, Substrate Specificity, and Inhibition of the Streptococcus Pneumoniae beta-ketoacyl-acyl Carrier Protein Synthase III (FabH). *J. Biol. Chem*. **2001**, *276* (32), 30024−30030.

(8) He, X.; Reynolds, K. A.; Purification, Characterization, and Identification of Novel Inhibitors of the Beta-ketoacyl-acyl Carrier Protein Synthase III (FabH) from Staphylococcus aureus. *Antimicrob. Agents Chemother*. **2002**, *46* (5), 1310−1318.

(9) Qiu, X.; Janson, C. A.; Konstantinidis; A. K.; Nwagwu, S.; Silverman, C.; Smith, W. W.; Khandekar, S.; Lonsdale, J.; and Abdel-Meguid, S. S. Crystal Structure of β-Ketoacyl-Acyl Carrier Protein Synthase III. *J. Biol. Chem.* **1999**, *274*, 36465−36471.

(10) Davies, C.; Heath, R. J., White, S. W.; and Rock, C. O. The 1.8 Å Crystal Structure and Active-site Architecture of Beta-ketoacyl-acyl Carrier Protein Synthase III (FabH) from *Escherichia coli*. *Structure* **2000**, *8*, 185−195.

(11) Scarsdale, J. N.; Kazanina, G.; He, X.; Reynolds, K. A.; Wright, H. T. Crystal Structure of the Mycobacterium Tuberculosis Beta-ketoacyl-acyl Carrier Protein Synthase III. *J. Biol. Chem.* **2001**, *276* (23), 20516−20522.

(12) Qiu, X.; Janson, C. A.; Smith, W. W.; Head, M.; Lonsdale, J.; Konstantinidis; A. K.; Refined Structures of Beta-ketoacyl-acyl Carrier Protein Synthase III. *J. Mol. Biol.* **2001**, *307* (1), 341−356.

(13) Lipinski, C. A.; Lombardo, F.; Dominy, B. W.; Feeney, P. J. Experimental and Computational Approaches to Estimate Solubility and Permeability in Drug Discovery and Development Settings. *Adv. Drug Delivery Rev.* **1997**, *23*, 3−25.

(14) Rishton, G. M. Reactive Compounds and In Vitro False Positives in HTS. *Drug Discovery Today* **1997**, *2*, 382−384.

(15) McGovern, S. L.; Caselli, E.; Grigorieff, N.; Shoichet, B. K. A Common Mechanism Underlying Promiscuous Inhibitors from Virtual and High-throughput Screening. *J. Med. Chem.* **2002**, *45*, 1712−1722.

(16) Wrobel, J.; Green, D.; Jetter, J.; Kao, W.; Rogers, J.; Perez, M. C.; Hardenburg, J.; Deecher, D. C.; Lopez, F. J.; Arey, B. J.; Shen, E. S. Synthesis of (bis)Sulfonic Acid, (bis)Benzamides as Follicle-Stimulating Hormone (FSH) Antagonists. *Bioorg. Med. Chem.* **2002**, *10*, 639−656.

(17) (a) Hassan, J.; Sevignon, M.; Gozzi, C.; Schulz, E.; Lemaire, M. *Chem. Rev.* **2002**, *102*, 1359−1470. (b) Miyaura, N.; Suzuki, A. *Chem. Rev.* **1995**, *95*, 7−2483.

(18) (a) Evans, D. A.; Katz, J. L.; West, T. R. Synthesis of Diaryl Ethers through the Copper-Promoted Arylation of Phenols with Arylboronic Acids. An Expedient Synthesis of Thyroxine. *Tetrahedron. Lett.* **1998**, *39*, 2937−2940. (b) Chan, D. M. T.; Monaco, K. L.; Wang, R. P.; Winters, M. P. New N- and O-Arylations with Phenylboronic Acids and Cupric Acetate. *Tetrahedron Lett.* **1998**, *39*, 2933−2936.

(19) Gajiwala, K. S.; Margosiak, S.; Lu, J.; Cortez, J.; Su, Y.; Nie, Z.; Appelt, K. Crystal structures of bacterial FabH enzyme from different species show significant differences in their substrate binding pockets. Manuscript in preparation.

(20) Flugel, R. S.; Hwangbo, Y.; Lambolot, R. H.; Cronan, J. E. Jr.; Walsh, C. T. Holo-(Acyl Carrier Protein) Synthase and Phosphopantetheinyl Transfer in *Escherichia coli*. *J. Biol. Chem*. **2000**, *275* (2), 959−968.

(21) Rock, C. O.; Cronan, J. E., Jr. Acyl Carrier Protein from *Escherichia coli*. *Methods Enzymol*. **1981**, *71*, 341−351.

(22) Otwinowski, Z.; Minor, W. Processing of X-ray diffraction data collected in oscillation mode. *Methods Enzymol.* **1997**, *276*, 307−326.

JM049141S